FREE FATTY ACIDS LIBERATED BY LIPOPROTEIN LIPASE MODULATE MACROPHAGE CHOLESTEROL EFFLUX VIA AKT ACTIVATION *IN VITRO*

by Jenika D. Marshall, B.Sc.

A dissertation submitted

to the School of Graduate Studies in partial fulfillment of the

requirements for the degree of

Master of Science

Department of Biochemistry

Memorial University of Newfoundland

May 2019

St. John’s, Newfoundland and Labrador

Abstract

Lipoprotein lipase (LPL) is upregulated in atherosclerotic lesions and it may promote the progression of atherosclerosis, but the mechanisms behind this process are not completely understood. My laboratory has previously shown that the phosphorylation of protein kinase B (Akt) within THP-1 macrophages is increased in response to the lipid hydrolysis products generated by LPL from total lipoproteins. Notably, the free fatty acid (FFA) component was responsible for this effect. I hypothesized that activation of Akt may play a role in cellular lipid accumulation. My results show that the total FFA component results in Akt phosphorylation in a dose-dependent manner over 18 hours. Specifically, palmitoleate can significantly increase Akt phosphorylation over two hours versus control. Additionally, I expanded previous studies showing that the total FFA component significantly inhibits cholesterol efflux to apolipoprotein (apo) A-I. I further show that blocking of Akt phosphorylation using the inhibitor MK-2206 restores cholesterol efflux levels to those observed for apolipoprotein A-I alone, for cells treated with either the total complement of FFA or palmitoleate alone. Overall, my data support a negative role for LPL in macrophage lipid accumulation, which is a major contributor to atherogenesis.

Acknowledgements

First, and most importantly, I wish to thank Dr. Robert Brown. He has been an excellent teacher and supervisor, and his guidance and support have been invaluable. I would like to thank my supervisory committee, Dr. Mark Berry and Dr. John Robinson, for their advice and insightful contributions to this work, as well as for their critical and thorough review of this manuscript. Over the past several years, I have been lucky enough to have many lab mates who have contributed to a truly positive and productive environment. I would like to thank all of them, especially those whose previous work led to this project, and those who helped to teach me the techniques I would use to produce it. I would also be remiss if I did not thank those at home who supported me without question every step of the way, including my parents, siblings, friends, and wonderful partner.

Table of Contents

List of Tables

List of Figures

List of Abbreviations

A/A	Antibiotic/antimycotic
ABCA1	Adenosine triphosphate-binding cassette transporter 1
ABCG1	Adenosine triphosphate-binding cassette transporter G1
Apo	Apolipoprotein
ATP	Adenosine triphosphate
CD36	Cluster of differentiation 36
CoA	Coenzyme A
CVD	Cardiovascular disease
DMSO	Dimethyl sulfoxide
EL	Endothelial lipase
FAF-BSA	Fatty acid-free bovine serum albumin
FBS	Fetal bovine serum
FFA	Free fatty acid
GPCR	G-protein coupled receptor
GPI	Glycosylphosphatidylinositol

GPIHBP1	Glycosylphosphatidylinositol-anchored high -density lipoprotein-binding protein 1
HEK	Human embryonic kidney
HL	Hepatic lipase
HMG	β-hydroxy β-methylglutaryl
IDL	Intermediate-density lipoprotein
LDL	Low-density lipoprotein
LMF1	Lipase maturation factor 1
LPL	Lipoprotein lipase
LXR	Liver X receptor
mTORC	Mammalian target of rapamycin complex
MUFA	Monounsaturated fatty acid
NF-κB	Nuclear factor κB
oxLDL	Oxidized low-density lipoprotein
PBS	Phosphate-buffered saline
PDK1	Phosphoinositide-dependent kinase 1
PI3K	Phosphoinositide 3-kinase
PIP2	Phosphoinositol bisphosphate

PIP3	Phosphoinositol triphosphate
PMA	Phorbol-12 myristate-13 acetate
PPAR	Peroxisome proliferator-activated receptor
PUFA	Polyunsaturated fatty acid
RIP3	Receptor interacting protein 3
RPMI	Roswell Park Memorial Institute
SDS-PAGE	Sodium dodecyl sulfate – polyacrylamide gel electrophoresis
SFA	Saturated fatty acid
SR-BI	Scavenger receptor class B type I
SREBP	Sterol regulatory element-binding protein
THL	Tetrahydrolipstatin
TNF-α	Tumor necrosis factor α
VLDL	Very low-density lipoprotein
VSMC	Vascular smooth muscle cell

Chapter 1 Introduction

1.1 Atherosclerosis

1.1.1 Incidence and prevalence of atherosclerosis

Atherosclerosis is a progressive inflammatory disease of the vascular intima. It involves the deposition and accumulation of fatty plaque along the interior of major blood vessels, eventually leading to at least partial occlusion of those vessels. Symptoms of the disease often do not appear until it is in its later stages, at which time damage to the vessels and risk of plaque rupture are of primary concern [1]. Hypertension, and other associated risk factors such as high serum cholesterol are very prevalent in North American society. In Canada, the prevalence of hypertension is 23%, rising despite better disease management options [2, 3]. The latest Heart Disease and Stroke Statistics Report from the American Heart Association estimates that 31.1% of the world's adult population has hypertension, with high blood pressure associated with up to 37.5% percent of deaths [4]. In addition, nearly half of the adults in the United States over the age of 40 have high enough blood cholesterol levels to qualify them for statin therapy, though actual statin use is not nearly this high [4]. The incidence of disease and mortality rates due to cardiovascular disease (CVD) in most high-income countries have been decreasing as diagnosis and treatment have improved, but remain a significant financial burden, both from pressure on the healthcare systems, and in lost productivity [4 - 6]. Low- and middle-income countries on the whole have poorer records for age-adjusted mortality rates due to clinical atherosclerotic conditions, though they are decreasing over

time [5, 7]. Though improvements in diagnosis and care are being made, there remains a genuine need to better understand the etiology of atherosclerosis.

1.1.2 Overview of atherosclerosis

Atherosclerosis, or at least the knowledge that arteries can become occluded over time, has existed since the 1500's, when Leonardo Da Vinci described the thickening of arteries in the elderly [8]. A long-held, and still valid explanation for the onset of this disease involves the disturbance of blood flow at junction points in the vessels, causing a mechanical disturbance and triggering an inflammatory repair mechanism [8, 9]. Diet was not regarded as a factor until much later, in the early 1900's. The earliest references to the role of dietary lipid in this disease come from experiments on rabbits and dogs, where the feeding of fatty diets and/or pure "cholesterin" induced the disease, even in atherosclerosis-resistant dogs [10, 11]. The initial stages of atherosclerosis (the fatty streaks) begin to develop in early childhood (even as early as *in utero*) with the gradual deposition of lipid-laden cells such as macrophages and vascular smooth muscle cells (VSMCs) along the interior of the blood vessels [12, 13]. It is a largely inflammatory-mediated process, and as such, is associated with other conditions of chronic low-grade inflammation such as obesity and metabolic syndrome [14]. Indeed, C-reactive protein levels, traditionally used as an indicator of infection or chronic inflammatory disease such as arthritis, are now measured as a risk factor for heart disease [15].

Figure 1 shows a brief overview of the cellular changes associated with the vessel microenvironment during the onset and progression of atherosclerosis. Briefly, there are

Figure 1: Overview of the development of atherosclerosis

Monocytes are recruited to a site of local inflammation along the vascular endothelium of a large artery. Once inside the intimal space, the monocytes, responding to the inflammatory signals in their environment, may differentiate into macrophages. Macrophages, along with resident vascular smooth muscle cells (VSMCs), then begin to take up lipid (especially oxidized low-density lipoprotein (oxLDL)) and become lipid-laden foam cells. These foam cells contribute to the development of a fatty streak which eventually becomes a complex lesion. At this stage, VSMCs, structural proteins, and free lipid, along with foam cells and necrotic cellular debris form a large plaque in danger of rupture. When a plaque ruptures, it creates a thrombus which can travel through the circulation and produce a lethal cardiac event or stroke. Figure created in Microsoft PowerPoint 2016.

Figure 1

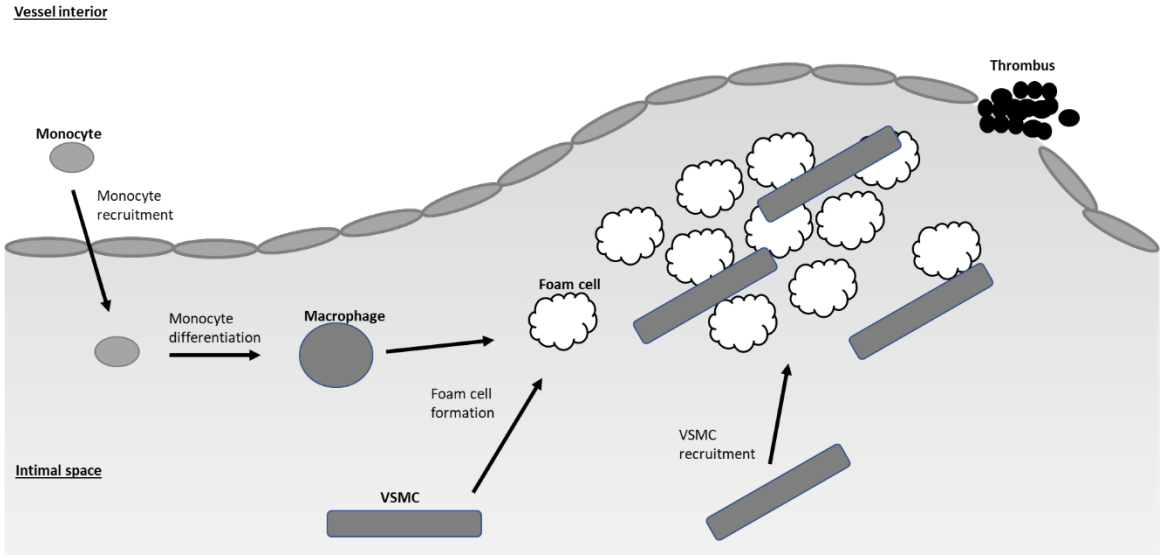
Vessel interior
Thrombus
Monocyte
Monocyte recruitment
Monocyte differentiation
Macrophage
Foam cell
Foam cell formation
VSMC recruitment
Intimal space
VSMC

several contributors to the early pathogenesis of this disease, including physical strain or insult to the vessel wall, poor dietary habits (such as a Western diet characterized by high fat and salt consumption, and low intake of fibre and omega-3 fatty acids), and oxidative stress in the microenvironment [16 - 18]. The extent to which each factor plays a role in the onset of this disease is debated. However, the progression once the disease is initiated is better understood. Macrophages within the intima of the blood vessels are largely responsible for the intake of excess lipid that results in the fatty streak. Some of these macrophages originate within the deeper structures of the vessel (the mesenchymal cells of the tissue), while many are recruited from the circulation as monocytes, which then differentiate into macrophages based on the environment within. Macrophages which take up excess lipid may differentiate further into foam cells, and begin secreting pro-inflammatory cytokines and chemokines, which stimulate the accumulation of foam cells [19]. The vessel wall will develop lesions consisting of foam cells, extracellular lipid, and some fibrous proteins before progressing to a complicated lesion where there is a necrotic core of dead cells within the plaque. This plaque can later become unstable and rupture, resulting in stroke or myocardial infarction [20]. Given the severe endpoints of this disease, it is crucial to continue investigating the contributing factors with an aim to better therapeutic options.

1.1.3 Lipoproteins

Before further discussing the development of atherosclerosis, it is important to understand how lipids travel through the circulation. While lipid is stored in cells in the form of specialized vesicles called lipid droplets, transport takes place in the form of

Figure 2: General lipoprotein structure

Lipoproteins are complexes of protein and lipid intended for the transport of lipid though the circulation. In order for this to occur, the largely non-polar lipids such as triglycerides and cholesteryl esters must be encased in a phospholipid monolayer. The phospholipids that make up the membrane are oriented such that the polar head groups are facing outward, and the non-polar tails inward. The membranes of lipoproteins also contain unesterified cholesterol and proteins. Figure created in Microsoft PowerPoint 2016.

Figure 2

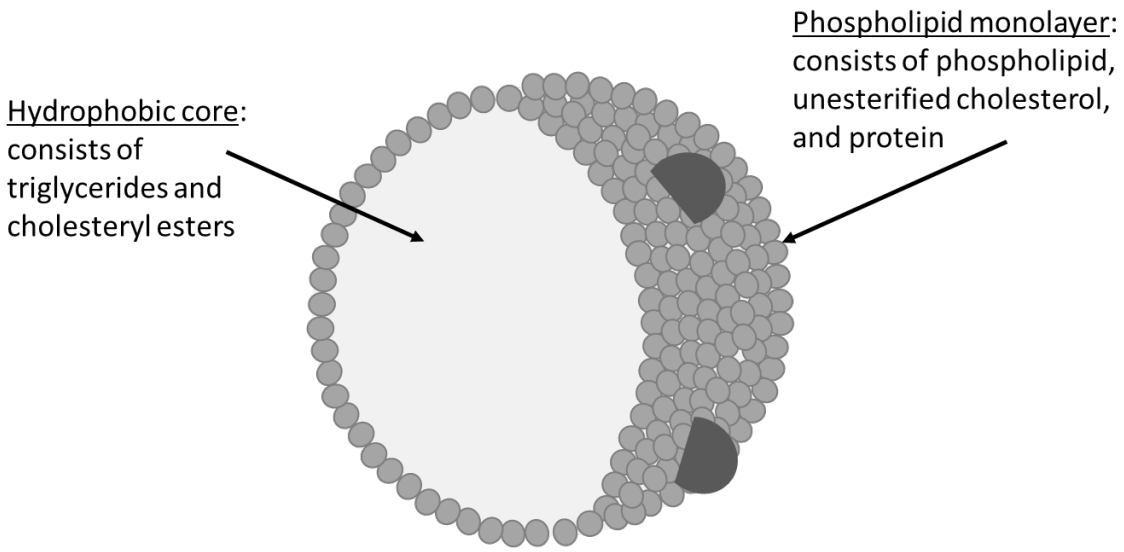
Phospholipid monolayer: consists of phospholipid, unesterified cholesterol, and protein
Hydrophobic core: consists of triglycerides and cholesteryl esters

lipoproteins. Lipoproteins are complexes of lipid contained in a phospholipid monolayer with embedded proteins, as shown in Figure 2. They are responsible for the transport of lipid through the circulation [21]. There are several classes and subclasses of lipoproteins, principally defined by particle density, origin, and function. The core of each lipoprotein consists of neutral lipids like cholesteryl esters and triglycerides, while the membrane consists of phospholipids and free cholesterol. Each lipoprotein is associated with one or more apolipoproteins (apo), which have a variety of functions including acting as cofactors and ligands [22]. These sealed lipid particles allow for the regulated transport and metabolism of lipid in the body.

Chylomicrons are the largest and least dense type of lipoprotein, and are derived from the diet. Each chylomicron is associated with one apoB48 that is synthesized in the small intestine and is required for chylomicron formation. In this form, chylomicrons first enter the lymphatic system, and then enter the circulatory system to transport dietary lipids to cells all over the body. Once the chylomicrons have been partially hydrolyzed by lipases such as lipoprotein lipase (LPL), they are known as chylomicron remnants. These remnants have had most of their triglycerides broken down, and are therefore smaller and more dense, with a higher ratio of cholesterol to triglyceride. Small dense lipoproteins are more atherogenic, with several studies identifying a positive association between an increase in the circulating levels of these lipoproteins and the development of CVD [23]. The remnants that are left in the circulation are delivered to the liver, where the remaining lipid is broken down. The liver then synthesizes very low-density lipoprotein (VLDL), which occurs in tandem with the synthesis of apoB100. VLDL are transported through the

circulation to distribute lipids to extrahepatic tissues, and in the process their lipids are hydrolyzed to form intermediate-density lipoprotein (IDL), and then low-density lipoprotein (LDL) [24]. Each of these three types of lipoproteins are always associated with one apoB100 – the same apoB100 that was synthesized along with the "parent" VLDL. Unlike all other apolipoproteins, which can be transferred and exchanged between lipoproteins, apoB proteins are non-exchangeable [25]. Chylomicrons, VLDL and IDL are also associated with apoE, a lipoprotein that facilitates the binding of these lipoproteins to cell surface receptors [24].

High-density lipoprotein (HDL) is the so-called "anti-atherogenic" lipoprotein. It is more dense than most, and it usually has a higher phospholipid and cholesterol content. Indeed, CVD risk is inversely associated with HDL levels according to several studies [26, 27]. HDL acts as a cholesterol acceptor, receiving cholesterol from extrahepatic tissues via cholesterol transporters such as adenosine triphosphate (ATP)-binding cassette subfamily G member 1 (ABCG1), ATP-binding cassette transporter 1 (ABCA1), and scavenger receptor-class B type I (SR-BI), and transporting the cholesterol back to the liver for excretion. The initial transfer of cholesterol from cells to HDL through these transporters is called cholesterol efflux. HDL are usually associated with at least one apoA-I protein and sometimes apoE as well [24]. It was postulated in 1979 that atherosclerosis is a "postprandial phenomenon", and it has been shown since that delayed clearance of chylomicrons, VLDL, and their remnants, is a risk factor for CVD [28, 29].

1.1.4 Atherosclerotic disease development and progression

Early atherosclerosis is typically an inflammatory response to increased lipid in the arterial space. LDL and VLDL are the primary lipoproteins found to influence this process, and these are typically elevated in the serum of individuals with metabolic syndrome and/or that follow a diet high in fat. When local inflammation is present in vessel walls, monocytes are recruited from the bloodstream to the site, where they differentiate into macrophages following environmental stimuli [30]. It is traditionally believed that the bulk of the macrophages in atherosclerotic plaques are derived from monocytes that have infiltrated the intima and differentiated near the plaque site. However, it has more recently been observed that macrophage proliferation within the plaque contributes more to the overall number [31]. Regardless of the manner in which macrophages become associated with the growing plaque, they contribute to disease progression in several ways. Plaque-associated macrophages demonstrate increased lipid accumulation, in part through an increase in the uptake of oxidized low-density lipoprotein (oxLDL), and the decreased capacity for cholesterol efflux. As macrophages, they are phagocytic in nature, and may begin taking up any excess lipids. In particular, they are shown to readily accept large quantities of oxidized lipid, such as that found in oxLDL, which arises when the lysine residues of apoB100 are modified and oxidized. Scavenger receptors such as cluster of differentiation 36 (CD36) are involved in the uptake of oxidized lipids and proteins [32]. In fact, it has been shown that when CD36 is missing from human monocytes, there is up to a 40% reduction of oxLDL uptake, highlighting the importance of scavenger receptors such as CD36 and SR-BI [33]. As the

lipid content of the cells increase they develop more lipid droplets and transition to the foam cell phenotype. Smooth muscle cells from the surrounding artery migrate to the plaque site and can develop a foam cell phenotype as well [34]. As the plaque begins to form, it is mostly comprised of fatty foam cells derived from macrophages and VSMCs. As the plaque development progresses however, extracellular lipid accumulates between the cells in the streak to form an intermediate, fibrous lesion containing both lipid and structural proteins like collagen [30]. At this point in the disease, there may be no outward signs of atherosclerosis beyond the presence of existing risk factors.

At this intermediate stage, the artery is significantly reduced in diameter due to the buildup of plaque, and further growth includes the incorporation of structural proteins, more smooth muscle cells, and the development of calcification. Blood pressure can be affected by the narrowing of the arteries at this stage, but the more critical end-points of the disease do not occur until the lesion becomes unstable. Studies have shown that individuals with more calcification present in atherosclerotic lesions have a significantly higher risk of a coronary event in the future, as it represents a more advanced plaque, and tends to make it less stable [35, 36]. During this stage, an increasing number of macrophage- and VSMC-derived foam cells begin to die. While normal cell death is not typically an issue that would lead to disease, apoptosis in this case can be damaging in the intermediate plaque due to the reduced ability to clear the cell debris from the local area. Both macrophages and VSMCs have been shown to produce reactive oxygen species within atherosclerotic lesions due to the presence of oxLDL, and this has further been proposed as a major mechanism by which these cells undergo apoptosis [37, 38]. However, this is not the only death pathway these lesion-associated cells follow,

especially as the lesion progresses to late-stage. Instead, they often necrose in an unregulated manner, or undergo the slightly more structured but still damaging necroptosis (or programmed receptor interacting protein 3 (RIP3)-dependent necrosis) death pathway [39]. In two mouse models of atherosclerosis, the *Ldlr*$^{-/-}$ and the *Apoe*$^{-/-}$ mice, a genetic knockout of *RIP3* reduced lesion area and the size of the necrotic core in later stages of the disease. This highlights the role of necrosis and necroptosis of foam cells in advanced plaque formation [40]. Inside the lesion space, the dead cells and debris accumulate from these death processes, causing the plaque to grow.

End stage atherosclerosis is characterized by an unstable fibrous cap, as the necrotic core grows and weakens, and the complicated lesion is at risk of breaking off as a thrombus. In the event that a thrombus does dislodge from the arterial wall, it can travel to a vital organ such as the brain or heart, resulting in severe injury or death [41].

1.2 Cholesterol efflux

1.2.1 Cholesterol metabolism in the body

Cholesterol is part of the sterol family of lipid biomolecules which is ubiquitous to all animal cells. It is a vital molecule for maintaining the dynamic structure of animal cell membranes, is involved in various cell signaling processes, and is a precursor for other important biomolecules such as bile [42, 43]. It is derived both from the diet and from *de novo* synthesis, which principally occurs in the liver and intestine [44].

Dietary cholesterol comes from animal products, as all animals are capable of synthesizing it, but plants can only do so to a much lesser extent. Instead, plants primarily

synthesize phytosterols, which have been shown to reduce LDL cholesterol by inhibiting intestinal uptake of dietary cholesterol [45]. Though cholesterol can be obtained through the diet (around 300 mg/day), it is not normally necessary to do so as most of the required cholesterol in the body is synthesized from acetyl-coenzyme A (CoA) (between 700 mg and 900 mg/day) [44]. In most countries, no recommended upper limit for cholesterol consumption exists (the US is an exception, with an UL of 300 mg/day), instead for lipids there is a more general recommendation that saturated and trans fat intakes stay below 10% of the total daily energy intake [46]. While regulations regarding dietary intakes are always evolving, the lack of specificity for cholesterol may be something to evaluate in the future.

While the majority of cholesterol synthesis in humans occurs in the liver and intestine, nearly all cells are capable of synthesis. The process starts with acetyl-CoA, a metabolite produced both from glycolysis and β-oxidation of fatty acids. The synthesis pathway is very long, requiring 18 ATP per molecule of cholesterol. Despite requiring many enzymes, the rate limiting step is the conversion of β-hydroxy β-methylglutaryl (HMG)-CoA to mevalonate by HMG-CoA reductase [42]. The main regulators of cholesterol synthesis in humans are the sterol regulatory element-binding protein (SREBP) transcription factors, which are master regulators of many genes of lipid metabolism, including those that code for HMG-CoA reductase, LDL receptor, and LPL [47].

One of the major functions of cholesterol is as a structural element in cell membranes. The presence of cholesterol in the lipid bilayer that defines most animal

membranes alters its structure and therefore its function. Cell membranes are not static structures; they grow and shrink as vesicles are either exocytosed or fused, the protein content changes as transporter and receptor expression fluctuates, and the lipids themselves that make up the bulk of cell membrane structure move, flip, and rearrange as needed [48]. The presence of cholesterol in the membrane causes the lipid chains inside the hydrophobic centre to be more ordered, which in turn regulates membrane permeability. It forms a central component of lipid rafts, dynamic domains in the cell membrane which are enriched in cholesterol and sphingolipids, and to which some proteins are targeted [49]. For example, glycosylphosphatidylinositol (GPI) linked proteins are more often found in complex with lipid rafts than in the less-ordered sections of cell membranes [50]. Lipid rafts tend to be in areas where signaling events take place, which is lost if the cholesterol content of the membrane is too low [49]. Cholesterol, aside from being an important structural component of cells, is a precursor for bile, vitamin D, and steroid hormones [44]. Cholesterol is therefore involved in a wide range of biological processes.

The primary location of cholesterol uptake, from either the diet or from bile is the small intestine, mediated by the Niemann-Pick C1-like 1 protein [51]. Once inside the body, it is transported by lipoproteins to the liver, and then to extrahepatic tissues. Excess cholesterol may be stored in adipocytes, though to some extent excess can be removed through an anti-atherogenic excretion route called reverse cholesterol transport.

1.2.2 Reverse cholesterol transport

Reverse cholesterol transport is the body's mechanism for recycling and excreting excess cholesterol. As discussed in the context of atherosclerosis, a large buildup of cholesterol and lipid within cells can become pathological so the system has adapted to allow for transfer of cholesterol from lipid-laden extrahepatic cells to high density lipoprotein for transport and excretion. Figure 3 shows an overview of the process of reverse cholesterol transport.

The first step in reverse cholesterol transport is called cholesterol efflux. This requires either apoA-I or an HDL particle to receive cholesterol from a macrophage via cholesterol transporters on the cell. ABCA1 is mainly responsible for the transport of cholesterol to apoA-I, resulting in the formation of nascent HDL, while ABCG1 and SR-BI are responsible for efflux to mature HDL [52].

Following cholesterol efflux, HDL brings the cholesterol to the liver via the circulation, where it can either be used for sterol biosynthesis, repackaging, or bile acid synthesis. The average rate of bile acid synthesis is approximately 500 mg per day, and once made, it is stored in the gallbladder until a meal is ingested. Postprandial release of bile acids into the intestine allows for the emulsification and absorption of dietary lipids, fat-soluble vitamins, and reuptake of free cholesterol. The cholesterol that is not re-absorbed in the intestine then gets excreted from the body through the feces [53]. While this process is anti-atherogenic, it is not sufficient to prevent the development of atherosclerosis, especially in the presence of a typical Western diet. Strategies to increase

Figure 3: Overview of reverse cholesterol transport

The first step of reverse cholesterol transport is the efflux of cholesterol from macrophages to apolipoprotein A-I (apoA-I) or high-density lipoprotein (HDL) via cholesterol transporters such as adenosine triphosphate (ATP)-binding cassette subfamily G member 1 (ABCG1), ATP-binding cassette transporter 1 (ABCA1), or scavenger receptor-class B type I (SR-BI). The HDL then travels through the circulation, delivering the cholesterol to the liver. In the liver, the cholesterol may be used for various functions, or may be used for the production of bile. The bile is then stored in the gall bladder until, after a meal, the bile is secreted into the small intestine to aid in digestion. Most cholesterol is reabsorbed through the small intestine, but that which is not is then excreted through the feces. Figure created in Microsoft PowerPoint 2016.

Figure 3

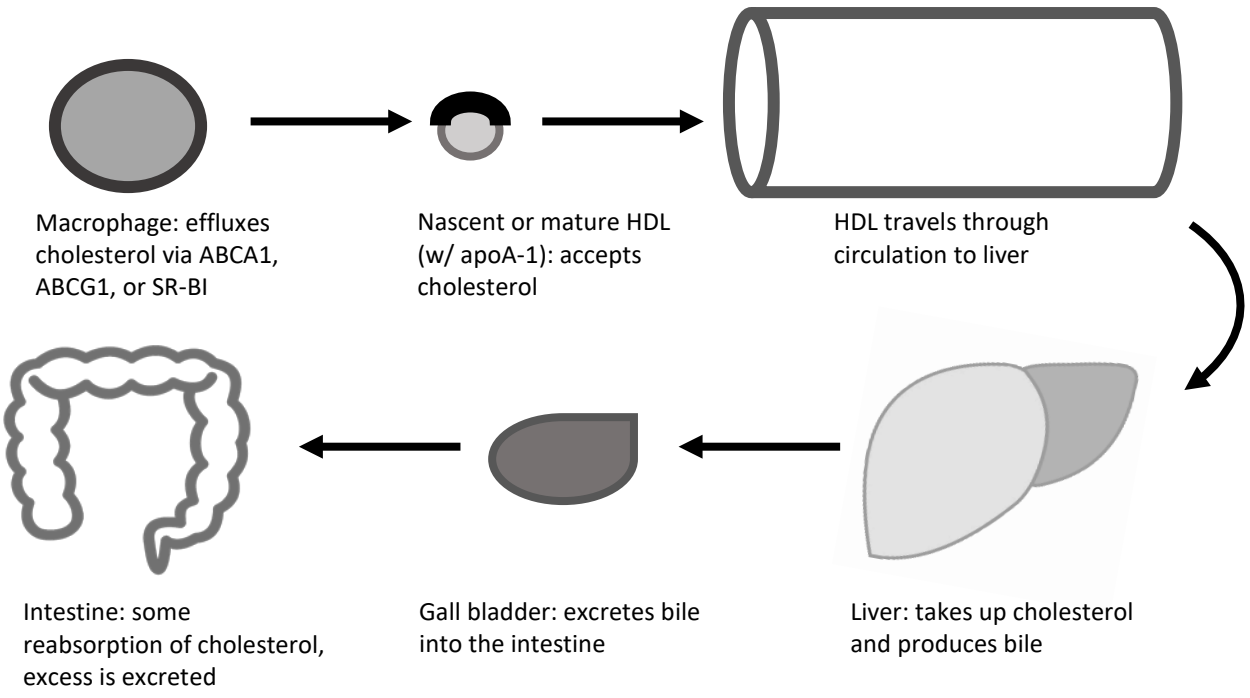
Macrophage: effluxes cholesterol via ABCA1, ABCG1, or SR-BI
Nascent or mature HDL (w/ apoA-1): accepts cholesterol
HDL travels through circulation to liver
Liver: takes up cholesterol and produces bile
Gall bladder: excretes bile into the intestine
Intestine: some reabsorption of cholesterol, excess is excreted

the capacity of reverse cholesterol transport are currently under investigation as a way to lower risk, and even as a potential therapeutic measure. While it is logical that an increase in HDL, the particle that accepts cholesterol for transport and eventual removal, should increase cholesterol clearance and reduce CVD risk, clinical trials to increase HDL in humans have been ineffective [54]. This does not disqualify HDL as a potential target for the treatment of atherosclerosis, but points to a need for further research in this area.

1.2.3 Macrophage cholesterol efflux

Cholesterol efflux from macrophages is the first step in the elimination of excess cholesterol. The levels of cholesterol in the body are very tightly regulated, and macrophage cholesterol efflux does not account for a large portion of the total body cholesterol at any point in time. However, given that macrophages (and their ability to store excess amounts of cholesterol) are a major causal factor in atherosclerosis, it almost certainly has an impact on the course of the disease [55]. It has been demonstrated that cholesterol efflux is compromised in serum from non-human primates that had advanced atherosclerotic lesions [52]. MicroRNAs are currently being studied as a target for increasing the cholesterol efflux capacity of macrophages in atherosclerotic plaques. MiR-33 is found in an intronic region of the *SREBF2* gene, and acts as a repressor of cholesterol transporter transcription, specifically ABCA1 and ABCG1. MiR-33 is expressed in macrophages, and its inhibition in *Ldlr*$^{-/-}$ mice (which are a mouse model of atherosclerosis) resulted in a reduction of plaque size, an increase in ABCA1 expression in plaque-associated macrophages, and enhanced cholesterol efflux [56]. These and other studies show that alteration of cholesterol efflux can affect the progression or

development of atherosclerosis, and may prove a valuable target in the treatment of the disease.

1.3 Lipoprotein lipase

1.3.1 The *sn*-1 family of lipases

Lipases consist of a group of enzymes that catalyze the breakdown of fatty acid-containing molecules such as triglycerides and phospholipids, releasing the fatty acids as single units for circulation. As such, they are important for a large variety of cellular functions, such as the maintenance of membrane dynamics, energy production, and signaling [57]. They are ubiquitous among all species of animals, and found at different concentrations in most tissues [58]. Many subcategories of lipase exist based on structure, substrate, and localization. The focus of this work is on a single lipase in the *sn*-1 family of neutral lipid lipases, which includes hepatic lipase (HL), endothelial lipase (EL), and LPL. These lipases are responsible for the hydrolysis of lipids such as triglycerides and phospholipids at the *sn*-1 position, and the subsequent release of free fatty acids (FFA), di- and mono-glycerides, and lysophospholipids. Figure 4 shows the general structure of a triglyceride and phospholipid with the *sn*-1 positions highlighted.

Of the *sn*-1 lipases, only LPL has a solved crystal structure. However, they are known to share significant sequence homology, and a recent phylogenetic divergence with each other and with pancreatic lipase, which has a solved structure [59]. Due to this, it is believed that all of the *sn*-1 lipases possess a ‘lid’ domain, along with the classical catalytic triad, which controls access to the active site [60]. These lipases also

Figure 4: *sn*-1 position of triglycerides and phospholipids

Basic structures of triglyceride and phospholipid are shown. *sn*-1 lipases are enzymes responsible for the cleavage of lipids from circulating lipoproteins and the delivery of the resultant hydrolysis products to the surrounding tissues. Lipase hydrolysis products may include free fatty acids, diacylglycerols, monoacylglycerols and lysophospholipids. The arrows in the figure indicate the *sn*-1 position that these lipases may target to remove the fatty acyl chain. Figure created in Microsoft PowerPoint 2016.

Figure 4

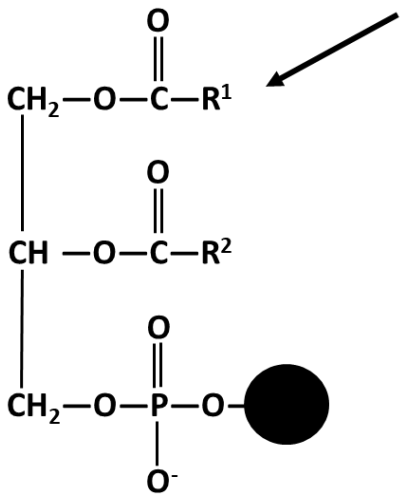

General phospholipid

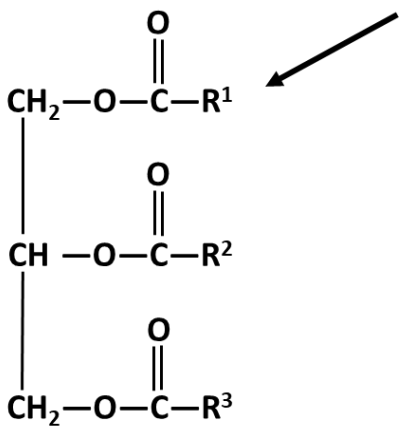

General triacylglycerol

display a non-catalytic bridging function which allows them to come into close contact with their substrates [61, 62]. This facilitates the enzymatic reaction and allows for more efficient uptake of the products, as well as acting as a regulatory mechanism.

Despite their similarities, these lipases have different tissue distribution and substrate specificities. EL is primarily located in the vascular endothelium, but is also found in the liver, lung, thyroid, testis, ovary, and placenta. It has a much more robust phospholipase activity than the other *sn*-1 lipases, and fairly low triglyceride lipase activity [60]. It is an important regulator of HDL cholesterol levels, as shown in studies using $EL^{-/-}$ mice where fasting plasma HDL cholesterol was increased by 57% [63]. Conversely, when overexpressed in mice, EL significantly reduces the levels of both HDL and apoA-1 [64].

HL hydrolyzes both phospholipids and triglycerides from various types of lipoproteins. This lack of apparent specificity is attributed to a slightly different lid domain structure. It is mainly synthesized in the liver, though can also be expressed in ovarian and adrenal tissues, and in macrophages [60]. HL can be pro- or anti-atherogenic depending on the model studied [60]. It plays a role in the hydrolysis and clearance of lipoprotein remnants, and it is through this anti-atherogenic function that HL has been investigated as a therapeutic target for the disease. Studies of HL overexpression in rats have shown improved clearance of remnant lipoproteins, as well as increased uptake of LDL [65]. Our laboratory has investigated the potential role of a protein mimicking the heparin-binding domain of HL as a way to displace more HL into the circulation, as an anti-atherogenic function [66].

1.3.2 Location and synthesis of LPL

LPL is an enzyme responsible for the hydrolysis of triglycerides from circulating chylomicrons and VLDL [67]. It is anchored to the outside of endothelial cells lining the luminal surface of capillaries in several tissues, including adipose, skeletal and cardiac muscle, and to a lesser extent, in macrophages, breast and adrenal tissues [68, 69]. While it is located on endothelial cells, it is mainly synthesized in the parenchymal cells of the respective tissues, with macrophages being an exception [70].

Like many proteins, it is synthesized in the endoplasmic reticulum in its monomeric form, at which point it is inactive. Lipase maturation factor 1 (LMF1) acts as a chaperone, facilitating the folding of the amino acid chain into the proper conformation [71]. LMF1 is essential for functional LPL (and HL) secretion, as evidenced by the combined lipase deficiency seen in both mice and humans with defects in the *Lmf1* gene [72]. The LPL monomers are then assembled into homodimers before being transferred to the Golgi for post-translational modifications like glycosylation [71]. After being heavily glycosylated, LPL is secreted into the interstitial space between cells in the tissue, then picked up by glycosylphosphatidylinositol-anchored high-density lipoprotein-binding protein 1 (GPIHBP1) and brought to the cell surface [73]. LPL that resides in the capillary space, linked to the outer cell membrane, is able to interact with its lipoprotein substrates.

1.3.3 Structure and function of LPL

The gene encoding human LPL is found on chromosome 8p22, and the fully translated monomer is 448 amino acids long [71]. The crystal structure of LPL (in complex with GPIHBP1) has been recently determined after years of study and the production of many predictive models [74, 75]. GPIHBP1 binds to and stabilizes the LPL protein in a 1:1 stoichiometry, and helps to prevent unfolding. LPL possesses a catalytic triad and lid domain similar to that of the previously solved pancreatic lipase. The active LPL enzyme is a homodimer in a head-to-tail orientation, with recent structural evidence suggesting that they may function *in vivo* as arrays [76, 77]. As stated before, LPL is located extracellularly, shuttled to the cell membrane by GPIHBP1 and attached to the outside by it and by heparan sulfate proteoglycans [73, 78, 79]. While LPL has basal activity, it is greatly enhanced by its co-activator, apoC-II [80]. ApoC-II is an exchangeable lipoprotein, found in complex with circulating triglyceride-rich lipoproteins including VLDL and chylomicrons [81]. Active LPL hydrolyzes the triglycerides residing in apoB-containing lipoproteins, as well as bridging the lipoproteins to the cell surface to allow for efficient uptake of the hydrolysis products. ApoC-I and apoC-III are negative regulators of LPL activity, disrupting the ability of LPL to bind to its substrate, and thus decreasing its activity [82]. Both of these apoproteins can be found on HDL, VLDL, IDL, and LDL, and are exchangeable [83].

1.3.4 Macrophage LPL

In addition to some major tissue types, macrophages also express LPL. Macrophages (and later foam cells) are responsible for the bulk of the accumulation of

lipid in the intimal space. As highly plastic cells, macrophages can rapidly adapt to their environment, thus it is not surprising to find that macrophages within atherosclerotic lesions display characteristics different from those located in normal tissue. Of note, it was first postulated by Zilversmit that macrophages in atherosclerotic lesions expressing LPL may be a contributing factor to the progression of atherosclerosis [84]. They discovered that macrophages within atherosclerotic plaques highly expressed LPL, and that LPL expression was positively correlated to the cholesterol content of the plaques [85]. In the decades since, the role of macrophage LPL in atherosclerosis has been further cemented. In *apoE*$^{-/-}$ mice, the transgenic expression of human LPL accelerated atherosclerotic lesion formation [86]. Conversely, when *apoE*$^{-/-}$ mice were treated with miR-590 (which can inhibit macrophage LPL expression), lesion formation was prevented [87]. Though all of the mechanisms by which macrophage LPL contributes to the pathogenesis of atherosclerosis are not yet known, it has roles in the production of pro-inflammatory cytokines, smooth muscle cell recruitment, and of course contributes to the lipid uptake of macrophages as part of their transition to foam cells [88 - 90].

1.4 Protein kinase B (Akt)

1.4.1 Akt structure and function

Protein kinase B, also commonly known as Akt, is a serine/threonine kinase involved in many cell signaling pathways [91]. It has three isoforms in humans, of which Akt1 is ubiquitously expressed in all tissues, Akt2 is found at its highest levels in insulin-responsive tissues, and Akt3 is mostly found in the brain [92]. The three isoforms are very similar in sequence and share three conserved domains: a pleckstrin homology

domain at the N-terminus responsible for membrane interactions, a catalytic kinase domain connected by a linker region, and a C-terminus putative regulatory domain characterized by a hydrophobic motif [93]. Akt1, which is the focus of this work, has two principal phosphorylation sites: Ser-473 in the regulatory region, and Thr-308 in the active site. Ser-473 is the best-studied and the site most commonly investigated when seeking to interrogate Akt function in most systems. Thr-308 must also be phosphorylated for full Akt activity, but the two sites are not acted on by the same kinase [94]. Akt itself is a kinase that can phosphorylate a variety of downstream proteins with a range of possible functions. One in particular that has been very well studied, and has been investigated in the context of atherosclerosis, is the mammalian target of rapamycin complex 1 (mTORC1). Akt phosphorylates tuberous sclerosis factor 2 (TSC2), which inactivates it, preventing it from inhibiting mTORC1. In the context of atherosclerosis, this has been shown to influence cholesterol efflux in mouse macrophages [95].

1.4.2 Phosphoinositide 3-phosphate signaling pathway

Akt is a downstream component of the class I phosphoinositide 3-kinase (PI3K) pathway, which begins with the activation of a receptor tyrosine kinase or G protein-coupled receptor (GPCR) on the cell surface. Following this, PI3K is induced to convert phosphatidylinositol bisphosphate (PIP2) to phosphatidylinositol triphosphate (PIP3). PIP3 then acts as a secondary lipid messenger, bringing Akt and its upstream kinases, phosphoinositide-dependent kinase 1 (PDK1) and the mTORC2 complex, from the cytosol to the cell membrane. PIP3 is able to interact with Akt though its pleckstrin homology domain. Following phosphorylation of Akt, it becomes active and may then

phosphorylate other proteins downstream [94]. Figure 5 shows a basic overview of PI3K signaling. It has been found that PI3K is more highly associated with lipid raft sections of the cell membrane, with signal transduction more strongly induced in these areas [96]. PI3K signals can be terminated by phosphatase and tensin homolog (PTEN) by dephosphorylating PIP3, regenerating PIP2 and releasing the downstream kinases from the cell membrane [97].

PI3K may be activated by a variety of stimuli, the most well studied of which include insulin and insulin-like growth factor-1. PI3K mediated responses to insulin have been implicated in the stimulation of lipogenesis in the liver [98]. It is a highly upregulated pathway in various types of cancers, often attributed to the involvement of Akt in the regulation of cell death and proliferation [97].

1.5 LPL hydrolysis products – previous findings and relevance

Of particular note, our laboratory has previously determined the subsets of various lipid species released from the hydrolysis of total human lipoproteins by LPL and EL. After treatment of THP-1 macrophages with these LPL hydrolysis products, it was found that several signaling nodes and receptor tyrosine kinases were activated, including Akt [99]. Further studies have shown that LPL hydrolysis products are able to differentially regulate expression of various genes and small nucleolar RNAs. More specifically, genes affecting cholesterol transport (*ABCA1*, *ABCG1*, *SCARB1*) were decreased, and genes affecting lipid storage (*CD36*, *PLIN2*) were increased [100, 101]. This has pointed to an overall pro-atherogenic role of LPL hydrolysis products in human macrophages, with

Figure 5: Overview of PI3K activation and downstream signaling

Phosphoinositide 3-kinase (PI3K) may be activated by a variety of receptor tyrosine kinases or G protein-coupled receptors (GPCRs). Following stimulation by a receptor, PI3K phosphorylates phosphatidylinositol bisphosphate (PIP2), converting it to phosphatidylinositol triphosphate (PIP3). PIP3 is a secondary lipid messenger that can interact with phosphoinositide-dependent kinase 1 (PDK1), mammalian target of rapamycin complex 2 (mTORC2), and Akt to bring them all to the cell membrane. PDK1 phosphorylates Akt at the Thr-308 site, while mTORC2 phosphorylates Akt at the Ser-473 site. Once fully phosphorylated, Akt can then interact with a variety of downstream targets. I hypothesize that FFA matching those released by the hydrolysis of total lipoproteins by LPL can influence Akt activation via incorporation the PIP signaling species. Further, that Akt activation can reduce the cholesterol efflux capacity of our THP-1 macrophages to apoA-I. Adapted figure courtesy of Ryan Elliott, created in Microsoft PowerPoint 2016.

Figure 5

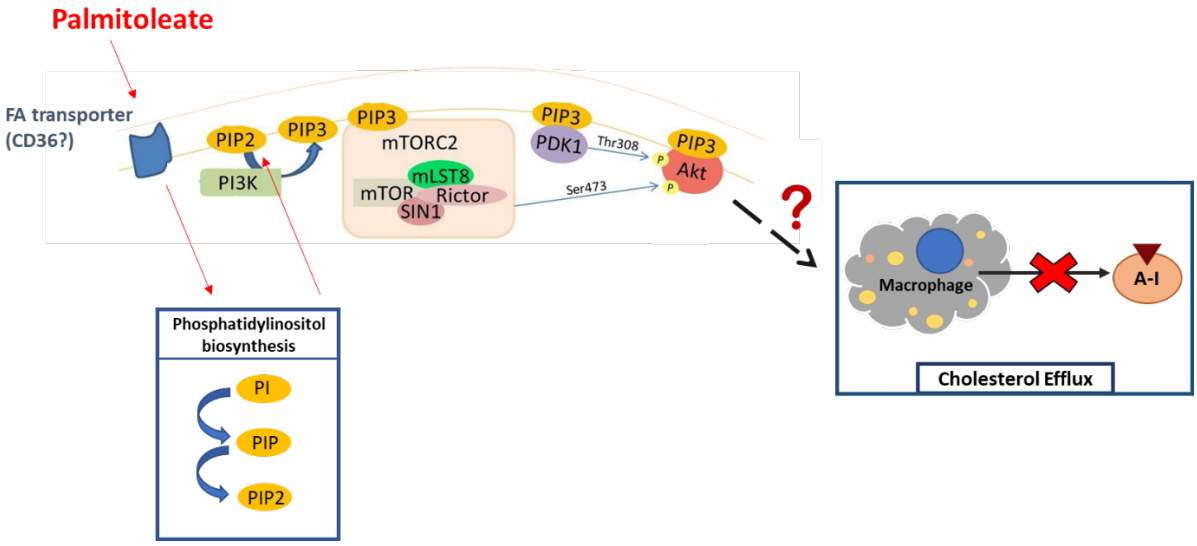
Palmitoleate
FA transporter
(CD36?)
PIP2
PIP3
PI3K
PIP3
mTORC2
mLST8
mTOR
Rictor
SIN1
PIP3
PDK1
Thr308
P
PIP3
Akt
P
Ser473
?
Macrophage
A-I
Cholesterol Efflux
Phosphatidylinositol
biosynthesis
PI
PIP
PIP2

likely effects on foam cell formation *in vivo*.

Aside from the entire complement of LPL hydrolysis products, treatment of THP-1 macrophages with the FFA component resulted in the activation of Akt [99]. This FFA subset has been shown to reduce cholesterol efflux to apoA-I in THP-1 macrophages and to increase the expression of pro-inflammatory cytokines [100]. To summarize, there is an increase in Akt activation on one hand, and pro-atherogenic cellular changes on the other hand, both in response to LPL hydrolysis products, and specifically the FFA component. Therefore, the question arises: are the two results connected? Preliminary and unpublished results from our laboratory show that the FFA subset of the LPL hydrolysis products can increase neutral lipid accumulation by 70% in our cells when compared to control, as determined by Oil-red O staining. When the same treatment was used along with the PI3K inhibitor LY294002 (as an upstream inhibitor of Akt), the lipid accumulation was reduced by 20%, indicating an effect of modulating the Akt pathway [Courage & Brown, unpublished]. While these data establish a link between LPL, Akt, and macrophage lipid, more questions remain as to how the FFA subset of the LPL hydrolysis products are activating Akt, and by what mechanisms this can affect macrophage function in the context of atherosclerosis.

1.6 Hypothesis

I hypothesize that the complement of FFA released by the hydrolysis of human total lipoproteins by LPL (as a reconstituted mixture) will activate Akt in a dose-dependent manner, and that specific FFAs in the total mixture may be responsible for the

effect. I further hypothesize that the ability of these FFA to reduce cholesterol efflux is at least partially mediated through Akt.

1.7 Objectives

Given that FFA released as LPL hydrolysis products have been shown to induce Akt phosphorylation in THP-1 macrophages, and to reduce cholesterol efflux in the same cells, the objectives of this project were 1) to determine more about how the FFA are activating Akt, and 2) to determine whether the reduction of cholesterol efflux may be moderated by Akt.

Chapter 2 Materials and Methods

2.1 Mammalian cell culture

2.1.1 THP-1 human monocyte cell culture

THP-1 human monocytic leukemia cells (#TIB-202, ATCC) were cultured in T75 flasks (BD Biosciences) with Roswell Park Memorial Institute (RPMI)-1640 medium containing 25 mM HEPES and 0.3 mg/L L-glutamine (#SH30255.01, Fisher), which was further supplemented with 10% v/v fetal bovine serum (#SH30396.03, Fisher) and 1% v/v antibiotic/antimycotic (A/A) (#15-240-062, Fisher). The cells were maintained at 37°C with 5% $CO_{2(g)}$ in an incubator. At 80-90% confluency, the cells were passaged by adding 2 mL of cell-containing media to a new flask containing 13 mL of the RPMI growth medium and incubated at 37˚C with 5% $CO_{2(g)}$.

2.1.2 THP-1 monocyte-to-macrophage differentiation

At 80 to 90% confluency, THP-1 cells were seeded for differentiation. From the confluent T75 flask, the cell-containing medium was transferred to a 15 mL tube for centrifugation. Cells were pelleted by spinning at 200 g for 5 minutes, after which the supernatant was removed and the cells resuspended in RPMI growth medium. Cells were counted using a hemocytometer (Fisher), and diluted to 3.86 x 10^5 cells per mL (or 7.72 x 10^5 cells per mL for gene expression analyses) in RPMI growth medium with 100 nM of phorbol 12-myristate 13-acetate (PMA) (#16561-29-8, Sigma) before seeding 2.5 mL in each well of a 6-well plate. Cells were allowed to incubate for 48 hours to differentiate

before being washed three times with plain RPMI and incubated with RPMI supplemented with 0.2% w/v fatty acid-free bovine serum albumin (FAF-BSA) (Fisher), 1% v/v A/A, and 100 nM PMA. Cells were incubated for 24 hours in this medium before treatments.

2.2 Treatment of THP-1 macrophages with FFA mixture

2.2.1 Preparation of FFA mixture

Purified FFA (Nu-Chek Prep) were kept as 10 mg/mL solutions in high performance liquid chromatography-grade methanol (Fisher), with treatment mixtures freshly prepared from these stocks prior to each experiment. For the total FFA mixture, final concentrations of each FFA matched those released and identified from the hydrolysis of total human lipoproteins by LPL (total FFA concentration of 0.68 mM), as seen in Table 1 [99]. Briefly, stock FFA were brought to room temperature and vortexed until uniform, then diluted in high performance liquid chromatography-grade methanol and pooled in a 1.5 mL centrifuge tube. In the case of treatments with only saturated fatty acids (SFA), myristate (14:0), palmitate (16:0), and stearate (18:0) were used; for monounsaturated fatty acids (MUFA), palmitoleate (16:1) and oleate (18:1) were used; for polyunsaturated fatty acids (PUFA), linoleate (18:2), arachidonate (20:4), and docosahexaenoate (22:6) were used. The contents of the tube were vortexed for 3 seconds before drying under $N_{2(g)}$ to remove the methanol. Prior to addition of FFA to treatment medium, they were dissolved in 30 μL of dimethyl sulfoxide (DMSO) (Sigma) and vortexed for 30 seconds. Stock solutions of FFA were stored in glass tubes under $N_{2(g)}$ at -20°C.

Table 1: Concentrations of FFA released from the hydrolysis of total human lipoproteins by LPL

Concentrations of free fatty acids (FFA) match those found following the hydrolysis of 3.9 mM (by phospholipid content) of total human lipoproteins by recombinant human lipoprotein lipase (LPL), at 0.68 mM FFA, as previously described [99].

Table 1

FFA Species	Concentration (nmol/mL) Matching LPL Hydrolysis Products
Myristate	18.6
Palmitoleate	23.7
Palmitate	275
Linoleate	70
Oleate	241.8
Stearate	45.2
Arachidonate	0.9
Docosahexaenoate	0.4

2.2.2 Treatments of THP-1 macrophages

Following differentiation, and 24 hours of incubation with RPMI supplemented with 0.2% w/v FAF-BSA, 1% v/v A/A, and 100 nM PMA, cells were ready for treatment. The cells were washed with plain RPMI before being incubated for 1 hour with RPMI supplemented with 0.2% w/v FAF-BSA, 1% v/v A/A, 100 nM PMA and 25 μg/mL tetrahydrolipstatin (THL) (Sigma), a lipase inhibitor. FFA treatment media were prepared as above, in RPMI supplemented with 0.2% w/v FAF-BSA, 1% v/v A.A, 100 nM PMA and 25 μg/mL THL. Control cells were treated instead with an equal concentration of DMSO as a vehicle control in the same medium. Cells were incubated in treatment medium for 2 hours at 37°C, 5% $CO_{2(g)}$ before collection.

2.2.3 Lysis and collection of treated THP-1 macrophages

After cell treatments, plates of cells were placed on ice before removing and discarding treatment medium. Cells were washed three times with 2 mL of ice-cold phosphate-buffered saline (PBS) at pH 7.0. To each well of a 6-well plate, 450 μL of a working solution of Triton X-100 containing cell lysis buffer (#9803S, Cell Signaling Technology) supplemented with 0.1% v/v protease/phosphatase inhibitor (#5872S, Cell Signaling Technology) was added and allowed to sit for 15 minutes. Cells were then scraped into the lysis buffer and collected into 1.5 mL centrifuge tubes to be stored at -80°C.

Prior to use, the cell lysates were measured for overall protein concentration using a bicinchonic acid (BCA) Protein Assay kit (Fisher), according to manufacturers

instructions. Briefly, cell lysates were added to a 96 well plate along with BCA assay buffer, along with a standard curve of albumin (from 0 mg/mL to 2000 mg/mL), and incubated at 37°C for 30 minutes. The plate was then read using a Biotek Powerwave microplate reader (Fisher), using an endpoint read at 562 nm. From this assay, the protein concentration of each collected sample could be calculated to ensure equal loading of sample in future protein gels.

2.3 SDS-PAGE and western blot analysis

2.3.1 SDS-PAGE

Proteins were analyzed and separated by sodium dodecyl sulfide polyacrylamide gel electrophoresis (SDS-PAGE) in gels containing a 12% (w/v) resolving gel, and a 4% (w/v) stacking gel, using a stock of 29:1 acrylamide:bis-acrylamide (#A3574, Sigma). For each sample to be loaded into the gel, a 20 μL solution containing 5 μg of protein, 5 μL of a 4x sample solution (50% v/v glycerol, 6% v/v β-mercaptoethanol, 10% w/v SDS, and 0.01% w/v bromophenol blue), and deionized water was made in a 1.5 mL centrifuge tube. The samples were boiled for 6 minutes before being loaded into the wells of the gel. A running buffer of Tris-glycine-SDS (TGS) was used for each instance of SDS-PAGE, diluted from a 10xTGS stock (#161-0772, BioRad). Gels were run for ~50 minutes at 200V.

2.3.2 Western blotting and imaging

Following protein separation by SDS-PAGE, the proteins were transferred to nitrocellulose membranes in cold transfer buffer (TGS supplemented with 20% v/v methanol), at 350 mA at 4°C for 2 hours.

Following transfer, the membranes were blocked in a solution of Tris-buffered saline (TBS) at pH 7.4 containing 5% w/v BSA, 0.05% v/v Tween 20, and 0.05% w/v sodium azide, on a rocker at 4°C overnight. After blocking, the membranes were incubated with blocking solution containing the primary antibody of interest. For each experiment, the gels were run in duplicate so as to analyze Akt and pAkt in the same samples. So, for one gel, the blocking solution contained a 1:1000 dilution of total anti-rabbit Akt antibody (#9272, Cell Signaling Technology), and for the other, the blocking solution contained a 1:2000 dilution of anti-rabbit pAkt (Ser-473) antibody (#4060, Cell Signaling Technology). In some cases a different anti-rabbit pAkt antibody was also used: a 1:2000 dilution of pAkt (Thr-308) antibody (#2965S, Cell Signaling Technology). Additionally, an anti-mouse β-actin antibody was used at a dilution of 1:5000 (#NB600-501, Novus). Membranes were incubated with primary antibodies on a rocker at 4°C overnight. Following primary incubation, the membranes were then washed four times with a solution of TBS containing 0.05% v/v Tween 20, by rocking at room temperature between each wash. Membranes were then incubated for two hours on a rocker at room temperature with the secondary antibody solution, which consisted of TBS containing 5% BSA, 0.05% Tween 20, and either a 1:2000 dilution of donkey anti-rabbit antibody conjugated to horseradish peroxidase (#SA1-200, Fisher), or a 1:2000 dilution of donkey

anti-mouse antibody conjugated to horseradish peroxidase (#SA1-100, Fisher). Following incubation, membranes were washed twice with TBS containing 0.05% Tween 20, and a further two times with TBS, by rocking at room temperature.

Membranes were visualized using an ImageQuant LAS detection system (GE Healthcare) following development using the ECL Prime Western Blotting Detection Kit (GE Healthcare), according to manufacturers protocol. Exposure occurred at -25°C at the chemiluminescence setting, and the visualized bands analyzed using ImageJ software. Densitometries were determined and used for statistical analysis.

2.4 Cholesterol efflux analyses

2.4.1 Desalting of apolipoprotein A-I

The apolipoprotein A-I (apoA-I) (Cedarlane) was thawed on ice and spun briefly. A PD-10 desalting column (GE Healthcare) was prepared and equilibrated to PBS buffer. The apoA-I was added to the column, and the flow-through collected. One mL aliquots of PBS were added to the column, and each mL of flow-through was collected into a separate tube. The collected fractions were analyzed in a UV-vis diode array spectrophotometer (Agilent) using a quartz cuvette. Absorbance was assessed at 280 nm against a blank of 1xPBS. The protein-containing fractions were pooled, and the pooled absorbance was re-measured at 280 nm. This absorbance measurement was used to calculate the concentration of apoA-I in the buffer, using the Beer-Lambert Law equation:

$$A = \varepsilon X b X c$$

where A is the absorbance of the sample, ε is the molar absorptivity coefficient (being 1.23 mL/mg x cm), b is the path length (1 cm), and c is the concentration. The apoA-I was then aliquoted into 1.5 mL centrifuge tubes and stored at -20°C until needed.

2.4.2 Measurement of cholesterol efflux in THP-1 macrophages

THP-1 monocytes were seeded into 12-well plates following the same protocol as in section 2.2. Cells were allowed to differentiate under 100 nM PMA for 48 hours before cholesterol loading. The procedure for cholesterol efflux is similar to that which is previously described [102]. Briefly, the spent medium was removed from the differentiated macrophages, and replaced with 500 μL of RPMI supplemented with 1% v/v FBS, 1% v/v A/A, 100 nM PMA, and 1 μCi/mL [^{3}H]cholesterol (Perkins-Elmer). Cells were then allowed to incubate for 24 hours to allow the tritiated cholesterol to incorporate into the system. After 24 hours, the medium was removed and the cells washed twice with 750 μL of RPMI supplemented with 0.2% w/v FAF-BSA, 1% v/v A/A, and 100 nM PMA. The cells were then incubated for 5 hours with 500 μL of the same medium. Next, the spent medium was removed and replaced with 480 μL of RPMI supplemented with 0.2% w/v FAF-BSA, 1% v/v A/A, 100 nM PMA, and 25 μg/mL THL, and incubated for 1 hour. Next, this medium was replaced by 446 μL of the same medium, but containing either the FFA treatment (at the concentrations previously defined), the FFA treatment along with 1 μM of Akt inhibitor MK-2206 (Selleckchem), or a DMSO vehicle control. The cells were treated for 18 hours. Following FFA treatment, the cells were washed twice with 750 μL of RPMI supplemented with 0.2%

w/v FAF-BSA, 1% v/v A/A and 100 nM PMA, before adding 446 µL of the same medium ± 25 µg/mL apoA-I to each group. Cells were incubated for 6 hours before collection of medium and cell lysates.

Medium from each well was collected into a separate labelled scintillation vial, to which 554 µL of deionized water was added. To the dry cells, 500 µL of 0.2 M NaOH was added to each well and allowed to sit for 30 minutes to lyse the cells. This solution was then washed over each well vigorously to collect the cells off the bottom of the plate, and then put into a labelled scintillation vial. An additional 500 µL of 0.2 M NaOH was added to each well, washed briefly, and then added to the corresponding vial for that well. To every sample, 5 mL of Scintiverse BD Cocktail (Fisher) was added, the vials capped and inverted 20 times to mix, and then left overnight before reading on a Tri-Carb 2810 liquid scintillation counter (Perkins-Elmer).

Cholesterol efflux was calculated as follows:

$$\%\ cholesterol\ efflux = \frac{media[\,^3H]}{media[\,^3H] + cell[\,^3H]}\ X\ 100\%$$

2.5 Gene expression analyses of cholesterol-associated genes

2.5.1 RNA isolation

For gene expression, treatments were carried out largely as described in section 2.2, however, in addition to control and FFA-treated cells, for each replicate, a group of FFA-treated/Akt inhibited cells were included. For treatments with the Akt inhibitor,

MK-2206, a 1 μM dose was added to the treatment medium [103]. Cells were treated for 18 hours, in order to stay consistent with previous experiments.

At the end of the 18 hour incubation in treatment medium, the spent medium was removed, and a 1 mL aliquot of Trizol (Fisher) was added to each well. Cells were scraped into the Trizol before being collected to a 1.5 mL centrifuge tube. RNA was isolated as previously described [103]. Briefly, 200 μL of chloroform (Fisher) was added to each sample tube and mixed well. The tubes were centrifuged at 13800 g for 15 minutes at 4°C to separate the aqueous, organic, and protein layers. The RNA was collected as the upper aqueous phase, and it was transferred to a fresh tube containing 500 μL of isopropanol (Fisher) and incubated at room temp for 5 minutes. These tubes were then centrifuged a second time at 13800 g for 20 minutes at 4°C to pellet the RNA. After centrifugation, the supernatant was removed and discarded, being careful not to disturb the pellet. To each pellet, 1 mL of 75% ethanol was added and the tubes centrifuged at 7500 g for 5 minutes at 4°C. The supernatant was removed and discarded, with the tubes left open until all ethanol had evaporated. Each pellet was then gently resuspended in 20 μL of nuclease-free water, before reading the RNA concentration (at 260nm, also assessing 230nm and 280nm peaks) on a Nanodrop 2000 Spectrophotometer (Fisher), using nuclease-free water as a blank.

The isolated RNA samples were then treated for DNA contamination using a TURBO DNA-free kit (Invitrogen), according to manufacturer's instructions. Briefly, to 10 μL of a 200 ng/μL solution of RNA, 1 μL of DNase buffer and 1 μL of DNase was

added before spinning the tubes briefly to mix. They were then allowed to incubate at 37°C for 25 minutes, after which 1 µL of DNase inactivation reagent was added. The tubes were gently mixed at room temp for 5 minutes, and then centrifuged at 10000 g for 2 minutes. The supernatant was collected into fresh tubes and the DNA pellet discarded. The RNA concentration of each sample was determined using a Nanodrop 2000 Spectrophotometer, using nuclease-free water as a blank.

Agarose gels were used to assess RNA degradation both before and after treatment with the TURBO DNA-free kit. In each case, a 1% agarose gel in Tris-acetate-EDTA buffer (#BP13354, Fisher) was used, and bands visualized by ethidium bromide detection on a FluorChem HD2 system (Bio-Techne).

2.5.2 cDNA synthesis

cDNA synthesis was performed using an Eppendorf Mastercycler (Fisher). Master mixes for the reaction were made in advance and placed on ice. Master mix 1 contained (per sample): 1 µL of random primers (3 µg/µL) (# 48190-011, Fisher) and 0.5 µL of deoxyribonucleotide triphosphate mix (10 mM) (#R0191, Fisher). Master mix 2 contained (per sample): 2 µL of 5x first-strand buffer (#Y02321, Fisher), 1 µL of 0.1 M dithiothreitol, and 0.5 µL of RNaseOut (40 U/µL) (#10777-019, Fisher). Master mix 3 contained (per sample): 0.5 µL of M-MLV reverse transcriptase (200 U/µL) (#28025013, Fisher). For each reaction, 500 ng of RNA was diluted in 4.5 µL of nuclease-free water. The first phase using master mix 1 incubated the samples for 5 minutes at 65°C. The second phase (after adding master mix 2) incubated the samples for 2 minutes at 37°C.

Finally, following addition of master mix 3, the samples were incubated in the following cycle conditions: 25°C for 10 minutes, 27°C for 50 minutes, 72°C for 10 minutes, followed by an infinite setting of 4°C until the samples were retrieved. Following this, the concentration of the cDNA samples was quantified using a Nanodrop spectrophotometer, and they were stored at -20°C until use.

2.5.3 Quantitative PCR analyses

Quantitative PCR was performed on a BioRad CFX96 Touch Real-Time PCR Detection System paired to a C1000 Touch Thermal Cycler (BioRad). iQ SYBRGreen Supermix (BioRad) was used according to manufacturers instructions to quantify gene expression of *ABCA1*, *ABCG1*, and *SCARB1*, using β-actin as a reference gene [104]. For each reaction, 25 ng of cDNA was used and the conditions were as follows: 95°C for 3 minutes, followed by 40 cycles of 95°C for 15 seconds, 59.5°C for 15 seconds, and 72°C for 20 seconds. Each set of replicates was run on a plate with both the gene of interest and β-actin. Table 2 shows the PCR primer sequences used for the genes analyzed.

Expression for each gene was calculated and standardized to β-actin using the ΔΔCt mathematical model, following previous protocols in our laboratory and using previously determined primer pair efficiencies [100, 104].

2.6 Statistical analysis

Statistical analyses were performed using unpaired Student's t test or one-way ANOVA with Tukey's multiple comparison post-test, unless otherwise stated. Unless

otherwise stated, all data are given as mean ± SD, with significance assigned to differences with a $p<0.05$.

Table 2: Real time PCR primer sequences

Gene	Forward Primer	Reverse Primer
ABCA1 XM_005251780.1	5'- AAC GAG ACT AAC CAG GCA ATC- 3' Template: 1778 ……..……..…1798	5'- ACA CAA TAC CAG CCC AGA AC -3' Template: 1925……..……...1906
ABCG1 XM_005261209.1	5'- GAG GGA TTT GGG TCT GAA CTG- 3' Template: 1108……..……..1128	5'- CTG TTC TGA TCA CCG TAC TCG- 3' Template: 1197……..……1177
SCARB1 XM_005253637.1	5'- ATC CTC ACT TCC TCA ACG C-3' Template: 979……..……..997	5'- TTC ACA GAG CAG TTC ATG GG- 3' Template: 1108……..1089

Chapter 3 Results

3.1 Assessment of Akt phosphorylation following total FFA treatment

The first objective of this study was to confirm by immunoblot what had previously been detected via antibody array [99]. Namely, that the FFA released from the hydrolysis of total lipoproteins by LPL could induce the phosphorylation of Akt. THP-1 cells were cultured, differentiated, and treated with the total FFA mixture as per section 2.2. Following immunoblot analysis according to section 2.3, it can be seen that Akt (at the Ser-473 site) was significantly activated by our FFA treatment compared to the control DMSO treatment (Figure 6). The ratio of phosphorylated Akt (pAkt) to total Akt in the FFA treated group was over 200% of control, confirming that this effect can be detected using our immunoblotting method. In addition, there was no alteration of β-actin in response to my FFA treatment.

3.1.1 Effect of overall FFA concentration on Akt phosphorylation

I sought to see if this effect was a function of the concentration of FFA present in the mixture, and further if we had reached the maximal effect on Akt at the overall concentration of 0.68 mM FFA. To test this, I completed additional experiments, following the protocols listed in sections 2.2 and 2.3, except the overall concentration of FFA was varied as follows: 0.17 mM, 0.34 mM, 0.68 mM, and 1.36 mM FFA. I did find a dose-dependent effect of our FFA treatment on the phosphorylation of Akt, such that lower doses caused less activation than larger doses (Figure 7).

Figure 6: Akt phosphorylation following treatment of THP-1 macrophages with total FFA mixture

A + B) THP-1 macrophages were exposed to a mixture of purified free fatty acids (FFA) matching the concentrations released from the hydrolysis of total human lipoproteins by recombinant human lipoprotein lipase (LPL) (0.68 mM by FFA), or with a vehicle control for 2 hours. Cell lysates were collected and proteins separated by SDS-PAGE, before being transferred to nitrocellulose and used for immunoblotting with densitometry analysis. Data are expressed as the ratio of phosphorylated Akt to total Akt, as a percent of Control (mean ± SD, from five independent experiments). Statistical analysis was performed using Student's t-test with p=0.002 (**).

Figure 6

A)

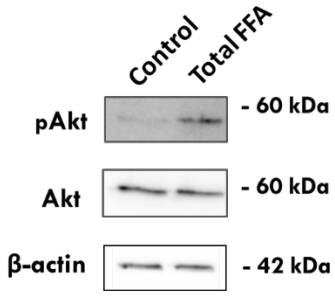
Control
Total FFA
pAkt
- 60 kDa
Akt
- 60 kDa
β-actin
- 42 kDa

B)

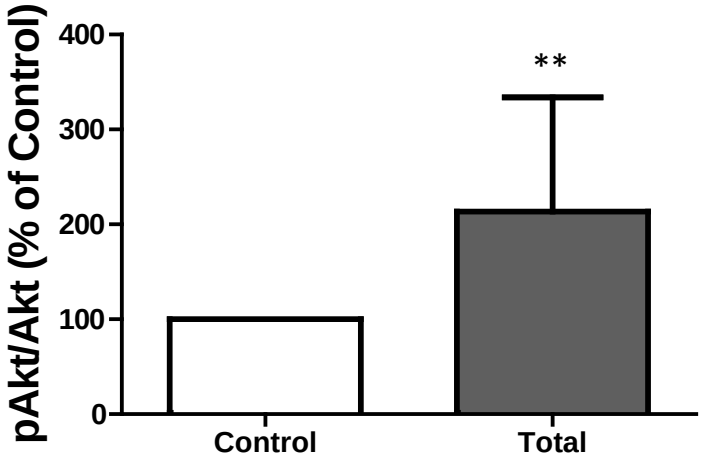
pAkt/Akt (% of Control)
400
300
200
100
0
**
Control
Total

Figure 7: Phosphorylation of Akt following treatment of THP-1 macrophages with varied doses of total FFA mixture

A + B) THP-1 macrophages were exposed to a mixture of purified free fatty acids (FFA) which are released from the hydrolysis of total human lipoproteins by recombinant human lipoprotein lipase (LPL) (0.17 mM, 0.34 mM, 0.68 mM, or 1.32 mM by FFA), or with a vehicle control for 2 hours. Cell lysates were collected and protein separated by SDS-PAGE, before being transferred to nitrocellulose and used for immunoblotting with densitometry analysis. Data are expressed as the ratio of phosphorylated Akt to total Akt, as a percent of Control (mean ± SD, from three independent experiments). Statistical analysis was performed using non-linear regression, with R^2=0.49, p=0.01.

Figure 7

A)

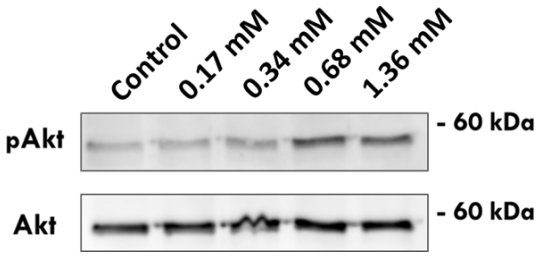
Control
0.17 mM
0.34 mM
0.68 mM
1.36 mM
pAkt
- 60 kDa
Akt
- 60 kDa

B)

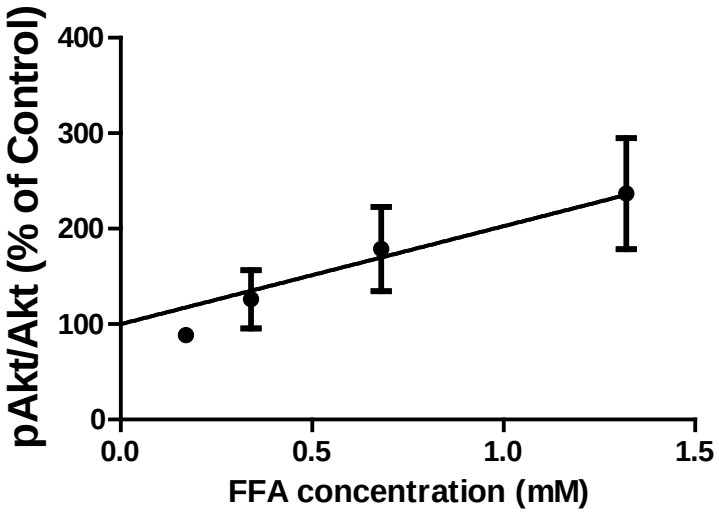
pAkt/Akt (% of Control)
400
300
200
100
0
0.0
0.5
1.0
1.5
FFA concentration (mM)

Additionally, the 1.36 mM dose of FFA increased FFA activation beyond our physiological dose of 0.68 mM. Thus, a statistically significant positive correlation between the overall concentration of our FFA mixture and Akt activation in THP-1 macrophages was observed.

3.2 Effect of varying FFA treatment time on Akt phosphorylation

In addition to changing the dose of FFA given to the THP-1 macrophages, I chose to alter the treatment time, in part to see how lasting the effects of our FFA are, but also to give some small insight to mechanism of activation. Protocols in sections 2.2 and 2.3 were followed, with the exception that treatment times were varied from 10 minutes to 18 hours. All other conditions were kept the same. Figure 8 shows these data for the Ser-473 site of Akt. We are able to see that maximal activation of Akt at this site seems to occur at approximately 20 minutes, though it remains above control levels even up to 18 hours. We see that activation begins at 10 minutes, indicating a relatively quick response to the FFA once added to the cells. The level of phosphorylation gradually decreases over time, but Akt does remain active at this principal site up to and possibly beyond 18 hours of treatment.

3.2.1 Effect of FFA treatment on Thr-308 phosphorylation

I investigated the other main phosphorylation site of Akt in response to the FFA treatment, Thr-308. The same samples analyzed for section 3.2 were instead probed with an antibody specific to Thr-308 and densitometry analysis was performed. Figure 9

Figure 8: Phosphorylation of Akt at Ser-473 following treatment of THP-1 macrophages with total FFA mixture at various time points

A + B) THP-1 macrophages were exposed to a mixture of purified free fatty acids (FFA) matching the concentrations released from the hydrolysis of total human lipoproteins by recombinant human lipoprotein lipase (LPL) (0.68 mM by FFA), or with a vehicle control for a range of time points. Cell lysates were collected and proteins separated, before being transferred to nitrocellulose and used for immunoblotting with densitometry analysis. Data are expressed as the ratio of phosphorylated Akt to total Akt, as a percent of Control (mean ± SEM, from three independent experiments).

Figure 8

A)

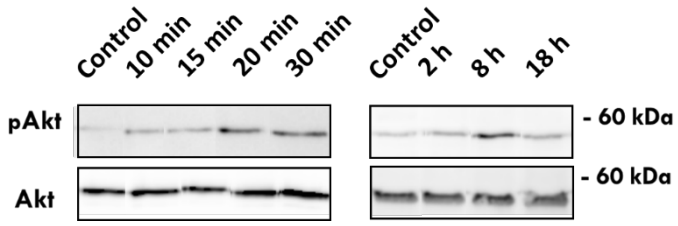
Control
10 min
15 min
20 min
30 min
Control
2 h
8 h
18 h
pAkt
Akt
- 60 kDa
- 60 kDa

B)

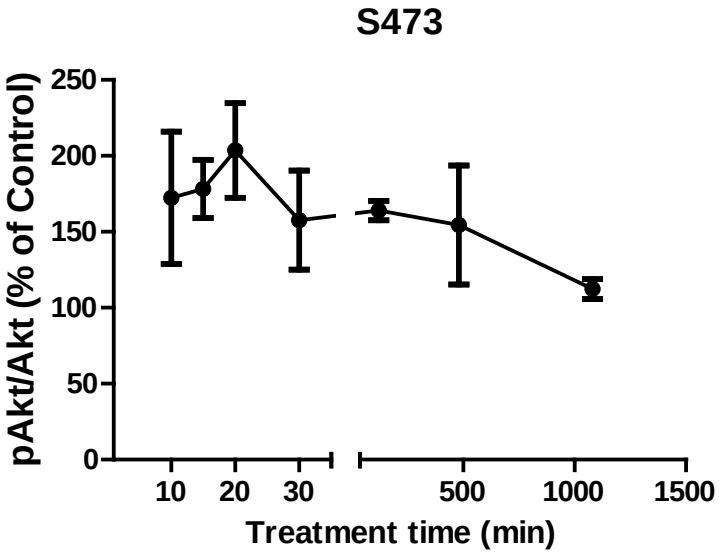
S473
pAkt/Akt (% of Control)
250
200
150
100
50
0
10
20
30
500
1000
1500
Treatment time (min)

Figure 9: Phosphorylation of Akt at Thr-308 following treatment of THP-1 macrophages with total FFA mixture at various time points

A + B) THP-1 macrophages were exposed to a mixture of purified free fatty acids (FFA) matching the concentrations released from the hydrolysis of total human lipoproteins by recombinant human lipoprotein lipase (LPL) (0.68 mM by FFA), or with a vehicle control for a range of time points. Cell lysates were collected and proteins separated, before being transferred to nitrocellulose and used for immunoblotting with densitometry analysis. Data are expressed as the ratio of phosphorylated Akt to total Akt, as a percent of Control (mean ± SEM, from three independent experiments).

Figure 9

A)

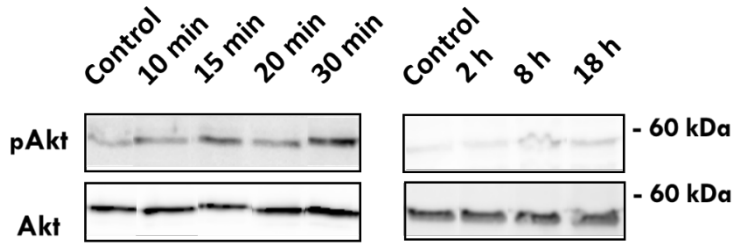
Control
10 min
15 min
20 min
30 min
Control
2 h
8 h
18 h
pAkt
Akt
- 60 kDa
- 60 kDa

B)

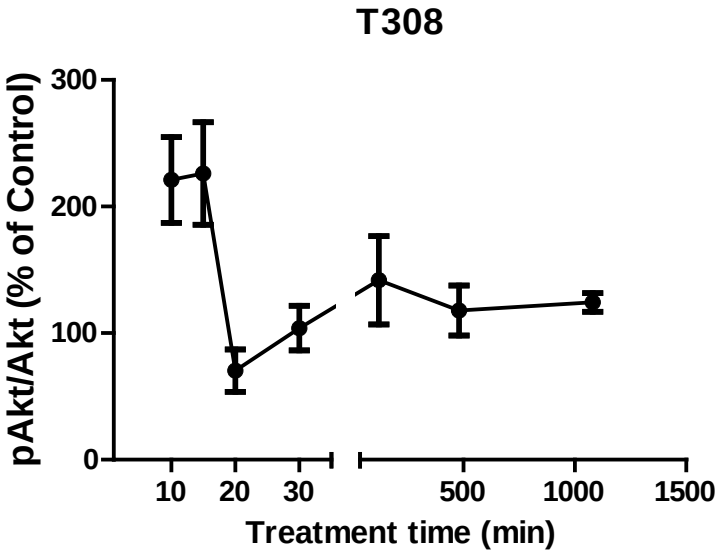
T308
pAkt/Akt (% of Control)
300
200
100
0
10
20
30
500
1000
1500
Treatment time (min)

shows that Akt activation was maximal at approximately 15 minutes, but the response was sharply decreased in the 20 minute treatment group. For all remaining time points, activation was apparently elevated in comparison, remaining slightly above control levels up to 18 hours. At most time points, levels of phosphorylation were lower for Thr-308 than for Ser-473.

3.3 Assessment of Akt phosphorylation following treatment with FFA of varying saturation

3.3.1 Effect of SFA, MUFA, and PUFA on Akt phosphorylation

Given the variety of FFA present in the overall mixture, and knowing that different FFA can have widely different effects as signaling molecules [105] [106] [107], it was important to determine if there were select FFA activating Akt. To start, I separated the FFA into three categories based on the saturation status of the carbon chain (or number of double bonds), 1) saturated fatty acids (SFA) myristate, palmitate, and stearate; 2) monounsaturated fatty acids (MUFA) palmitoleate and oleate; and 3) polyunsaturated fatty acids (PUFA) linoleate, arachidonate, and docosahexaenoate. Cells were treated as stated in sections 2.2 and 2.3, but with only the selected FFA of each group. Concentrations still matched those found in Table 1, so as to be physiologically relevant. From these treatments, only the MUFA treatment was able to statistically significantly elevate Akt phosphorylation beyond the control (Figure 10).

Figure 10: Akt phosphorylation following treatment of THP-1 macrophages with groups of FFA varied by saturation

A + B) THP-1 macrophages were exposed to mixtures of purified free fatty acids (FFA) matching the concentrations released from the hydrolysis of total human lipoproteins by recombinant human lipoprotein lipase (LPL) (0.68 mM by FFA), or with a vehicle control for 2 hours. Mixtures were as follows: Total (all FFA), saturated fatty acids (SFA - 14:0, 16:0, 18:0), monounsaturated fatty acids (MUFA - 16:1, 18:1), and polyunsaturated fatty acids (PUFA - 20:4, 22:6). Cell lysates were collected and proteins separated by SDS-PAGE, before being transferred to nitrocellulose and used for immunoblotting with densitometry analysis. Data are expressed as the ratio of phosphorylated Akt to total Akt, as a percent of Control (mean ± SD, from five independent experiments). Statistical analysis was performed using one-way ANOVA with Tukey's multiple comparison test, with p=0.02 (*) and p=0.006 (**) compared to Control.

Figure 10

A)

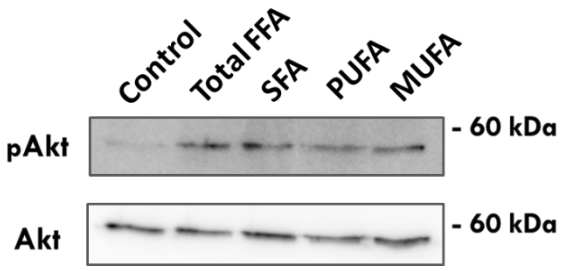
Control
Total FFA
SFA
PUFA
MUFA
pAkt
- 60 kDa
Akt
- 60 kDa

B)

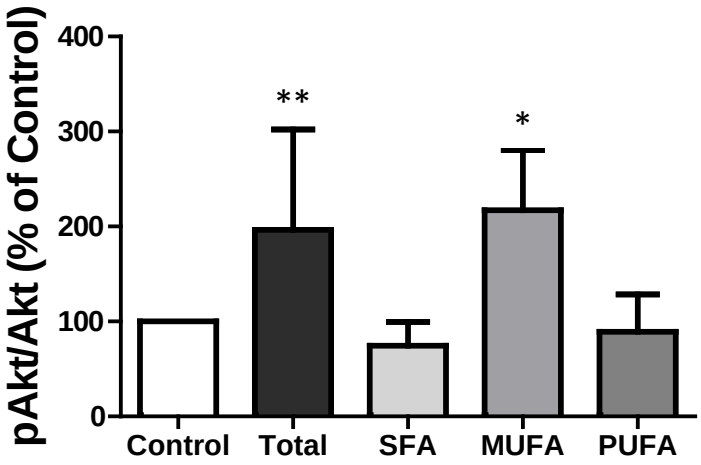
pAkt/Akt (% of Control)
400
300
200
100
0
**
*
Control
Total
SFA
MUFA
PUFA

3.3.2 Effect of individual MUFA on Akt phosphorylation

Given that MUFA was the class of FFA to have a significant effect on Akt activation, the two fatty acids in that class were used separately to determine if one or the other was having the significant effect alone. Therefore, THP-1 macrophages were treated as previously described, as per section 2.2 and 2.3, and at the concentrations listed in Table 1, with either palmitoleate (16:1), oleate (18:1), or a control. From this, we can see that only palmitoleate significantly increased Akt phosphorylation, indicating that this fatty acid is likely the driving force of the FFA component of the LPL hydrolysis products for Akt signaling (Figure 11).

3.4 Cholesterol efflux analyses following FFA treatment and Akt inhibition

3.4.1 Verification of Akt inhibition by MK-2206

In order to determine if any downstream effects of FFA treatment may be due to Akt, a means of inhibiting or blocking Akt was required. MK-2206 is a highly specific, allosteric chemical inhibitor of Akt that has not shown interactions with any other kinases. It works in the micromolar range for most cell types, and in my model I used a 1 μM concentration. Figure 12 shows a representative western blot of THP-1 cell lysates following treatment with MK-2206. At the 1 μM dose, there was no discernable pAkt band, indicating inhibition. There were no changes to β-actin expression.

Figure 11: Akt phosphorylation following treatment of THP-1 macrophages with distinct MUFA

A + B) THP-1 macrophages were exposed to either palmitoleate (16:1), oleate (18:1), or to a vehicle control for 2 hours. Free fatty acid (FFA) concentrations matched those of the same FFA released from the hydrolysis of total human lipoproteins by recombinant human lipoprotein lipase (LPL) (Table 1). Cell lysates were collected and protein separated by SDS-PAGE, before being transferred to nitrocellulose and used for immunoblotting with densitometry analysis. Data are expressed as the ratio of phosphorylated Akt to total Akt, as a percent of Control (mean ± SD, from five independent experiments). Statistical analysis was performed using a one-way ANOVA with Tukey's multiple comparison test, with p=0.006 (**) compared to Control.

Figure 11

A)

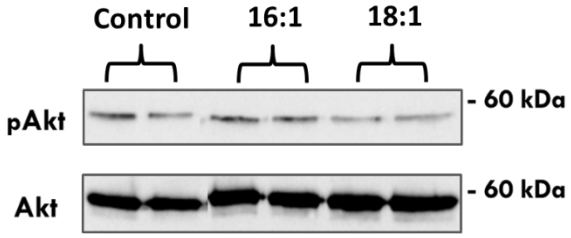
Control
16:1
18:1
pAkt
- 60 kDa
Akt
- 60 kDa

B)

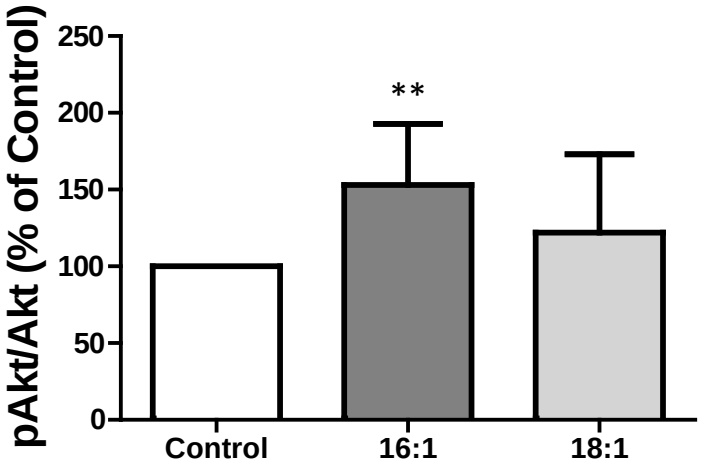
pAkt/Akt (% of Control)
250
200
150
100
50
0
**
Control
16:1
18:1

Figure 12: Representative image of a western blot for detection of pAkt following treatment of THP-1 macrophages with MK-2206

THP-1 macrophages were exposed to a 0.5 μM dose (0.5) and a 1 μM (1) dose of Akt inhibitor MK-2206, or vehicle controls (0.5C, 1C). Cell lysates were collected and used for immunoblotting, probing both Akt and pAkt. Inhibition was confirmed by a lack of pAkt band following treatment, indicating an inactive Akt.

Figure 12

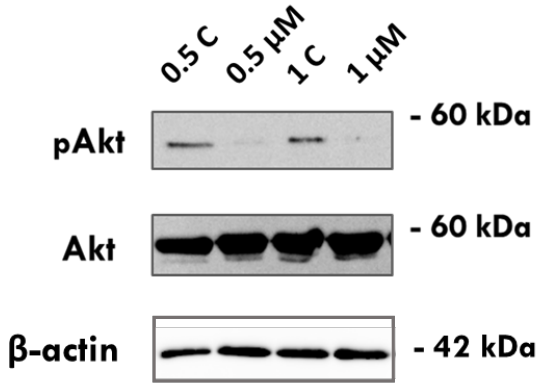

3.4.2 Cholesterol efflux to apoA-I following treatment with total FFA mixture and Akt inhibition

Previously, our laboratory has shown that an 18 hour treatment with our FFA mixture has reduced the THP-1 macrophages ability to efflux cholesterol [100]. In this study, I sought to determine if this process could be mediated through Akt. THP-1 macrophages were treated as per section 2.4. Figure 13 shows that, as expected, the FFA mixture decreased cholesterol efflux to apoA-I by almost 40% compared to control levels. When the cells were simultaneously treated with the Akt inhibitor MK-2206 however, efflux was restored, with no significant difference between the control group and the FFA plus inhibitor group.

3.4.3 Cholesterol efflux to apoA-I following treatment with palmitoleate or oleate and Akt inhibition

Given that other experiments have shown that palmitoleate (16:1) is likely the principal FFA to induce Akt phosphorylation, I sought to determine if it would reduce cholesterol efflux to apoA-I. The experiment was conducted as in section 2.4, and the results mirrored that of the total FFA experiments, as shown in Figure 14. When treated with palmitoleate (at the concentration seen in the LPL hydrolysis products), the THP-1 macrophages displayed a reduction in cholesterol efflux by approximately 30%

Figure 13: Cholesterol efflux to apoA-I in THP-1 macrophages in response to total FFA mixture and MK-2206 treatment

THP-1 macrophages labelled with [^{3}H]cholesterol were treated for 18 hours with the FFA mixture (FFA), the FFA mixture along with 1 μM MK-2206 (FFA+MK), or a vehicle control (Control), then subsequently tested for cholesterol efflux ability to apoA-I over 6 hours. Efflux was calculated as a percent of media [^{3}H]cholesterol per total cell and media [^{3}H]cholesterol. All data were corrected for control efflux experiments to 0.2% w/v FAF-BSA. Data are presented as mean ± SD from eight independent experiments. Statistical analysis was performed using one-way ANOVA with Tukey's multiple comparison test, with $p<0.05$ (*) and $p<0.001$(***).

Figure 13

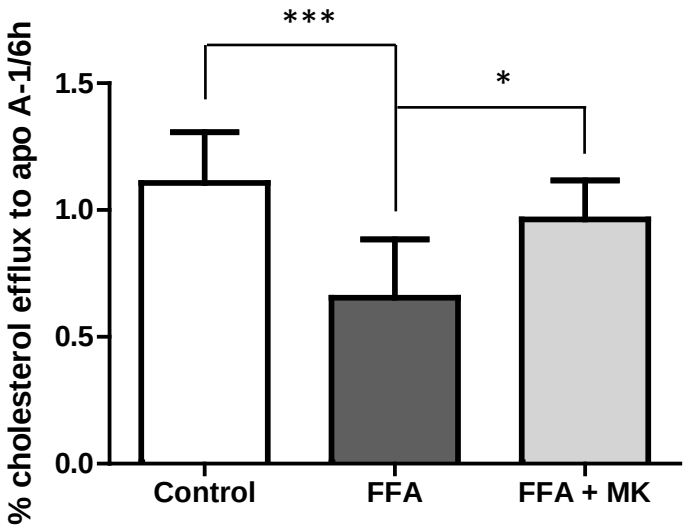

Figure 14: Cholesterol efflux to apoA-I in THP-1 macrophages in response to palmitoleate (16:1) and MK-2206 treatment

THP-1 macrophages labelled with [^{3}H]cholesterol were treated for 18 hours with palmitoleate (16:1), palmitoleate along with 1 μM MK-2206 (16:1+MK), or a vehicle control (Control), then subsequently tested for cholesterol efflux ability to apoA-I over 6 hours. Efflux was calculated as a percent of media [^{3}H]cholesterol per total cell and media [^{3}H]cholesterol. All data were corrected for control efflux experiments to 0.2% w/v FAF-BSA. Data are presented as mean ± SD from five independent experiments. Statistical analysis was performed using one-way ANOVA with Tukey's multiple comparison test, with $p<0.05$ (*).

Figure 14

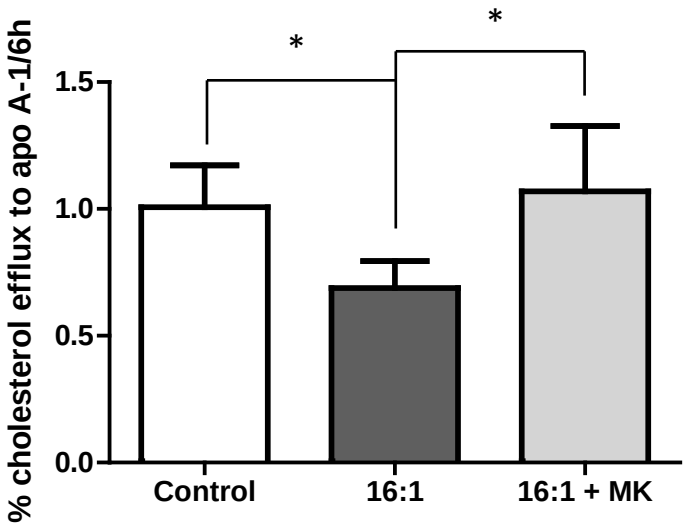

compared to control. Cells treated with the Akt inhibitor, however, showed efflux indistinguishable from control levels.

I repeated this experiment using oleate, to determine if 1) cholesterol efflux would be affected, and 2) if there would be any effect of the Akt inhibitor. Shown in Figure 15, I did find a non-significant reduction in cholesterol efflux to apoA-I in our THP-1 macrophages following treatment with oleate. There was no significant effect of the Akt inhibitor.

3.5 The effect of total FFA mixture and Akt inhibition on expression of cholesterol-associated genes

Given that the FFA mixture was reducing cholesterol efflux, in a manner that is affected by Akt phosphorylation, I decided to look into the expression of cholesterol transporter genes in THP-1 macrophages, and if perhaps inhibition of Akt might alter their expression profiles. To do this, I used previously validated primers for *ABCA1*, *ABCG1* and *SCARB1*, using β-actin as a control. Previously, our laboratory has shown that this FFA mixture was able to significantly reduce the mRNA expression of *ABCA1*, *ABGC1*, and *SCARB1* [100]. While a trend to a decrease could be seen with *ABCA1*, only *ABCG1* expression was significantly reduced by approximately 25% following our FFA treatment in this case (Figure 16). While this was unexpected, importantly for this experiment, the Akt inhibitor had no effect on any of the results, including *ABCG1*.

Figure 15: Cholesterol efflux to apoA-I in THP-1 macrophages in response to oleate (18:1) and MK-2206 treatment

THP-1 macrophages labelled with [^{3}H]cholesterol were treated for 18 hours with oleate (18:1), oleate along with 1 μM MK-2206 (18:1+MK), or a vehicle control (Control), then subsequently tested for cholesterol efflux ability to apoA-I over 6 hours. Efflux was calculated as a percent of media [^{3}H]cholesterol per total cell and media [^{3}H]cholesterol. All data were corrected for control efflux experiments to 0.2% w/v FAF-BSA. Data are presented as mean ± SD from five independent experiments. Statistical analysis was performed using one-way ANOVA with Tukey's multiple comparison test, with n.s.

Figure 15

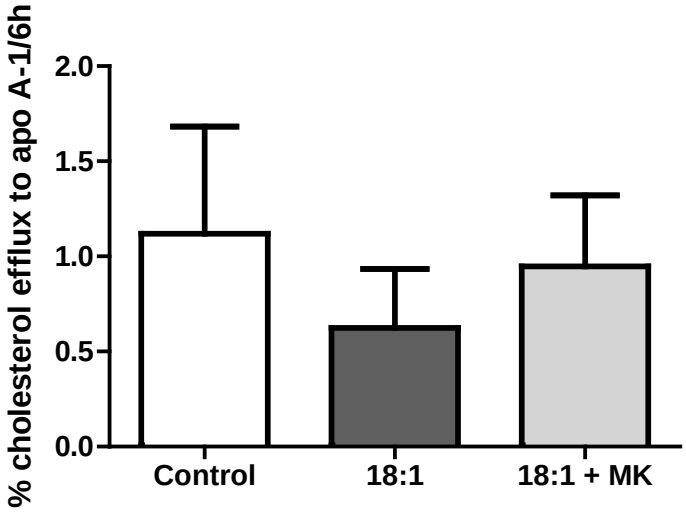
% cholesterol efflux to apo A-1/6h
2.0
1.5
1.0
0.5
0.0
Control
18:1
18:1 + MK

Figure 16: Analysis of gene expression levels of cholesterol transporter genes in THP-1 macrophages incubated with total FFA mixture and MK-2206

THP-1 macrophages were treated with either total FFA mixture (FFA), FFA with MK-2206 (FFA + MK), or a vehicle control (Control) for 18 hours. RNA was collected, and real-time PCR was performed on the samples using primers for A) *ABCA1*, B) *ABCG1*, and C) *SCARB1*. All results are presented as means ± SD (from four independent experiments) as a percentage of the control gene expression, normalized to β-actin. Statistical analyses were performed using one-way ANOVA with Tukey's multiple comparison test, with p=0.04 (*).

Figure 16

A)

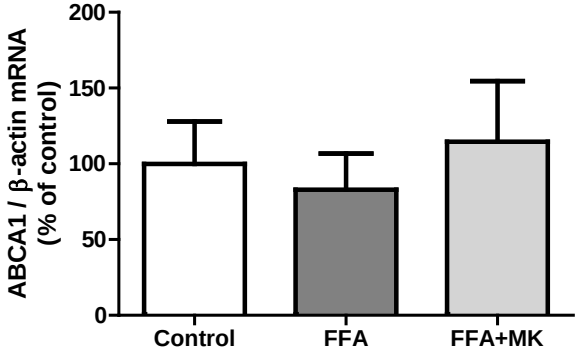

B)

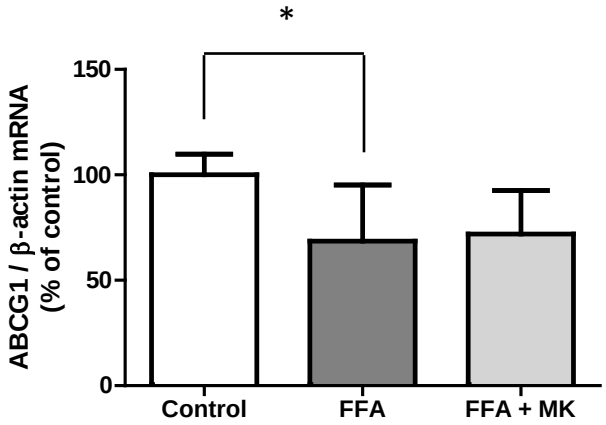

C)

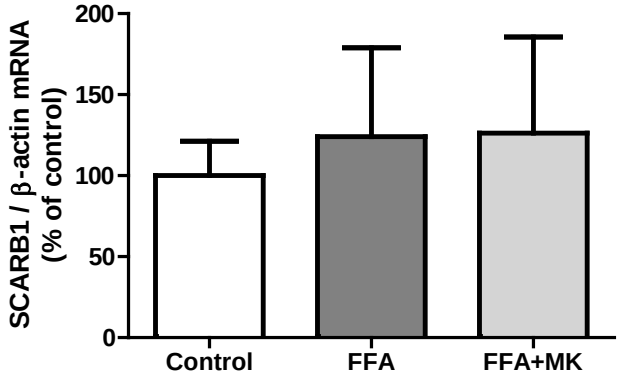

Chapter 4 Discussion

4.1 Dose-dependent ability of purified FFA released by LPL to moderate Akt activity

Beyond their roles as energy sources and structural lipids, FFA are potent signaling molecules. They act as endogenous ligands for nuclear receptors such as peroxisome proliferator-activated receptors (PPAR), liver X receptor (LXR), SREBP, nuclear factor κB (NF-κB), in addition to Toll-like receptors and GPCRs [106]. While it could be expected that these lipids would influence processes associated with lipid metabolism, FFA, through regulation of some of these receptors, are able to play a role in more diverse functions, such as glucose metabolism through PPARs [108 - 110], and cytokine release through NF-κB [111], in addition to processes like *de novo* lipogenesis and cholesterol metabolism [112, 113].

In our laboratory, we have confirmed a role for our FFA mixture in decreasing the gene expression of nuclear receptors PPARα, PPARγ and LXRα in THP-1 macrophages [100], as well as increasing the expression of the pro-inflammatory cytokine tumor necrosis factor-α (TNF-α) [101]. Previously, we have shown that Akt is significantly phosphorylated by our FFA mixture through the use of antibody arrays, and I sought to verify its detection by immunoblotting [99]. As expected, I found a statistically significant phosphorylation of Akt following these treatments (Figure 6). Akt is a master kinase, with over 100 unique downstream substrates, and clearly defined roles in a variety

of functions, such as cell growth and proliferation, insulin response, and angiogenesis [91]. As such, there are a myriad of pathways that could be influenced by a change in Akt phosphorylation status, some of which have implications in atherogenic processes. An example of this has been demonstrated by showing the influence of Akt on TNFα-mediated expression of monocyte chemoattractant protein-1, a protein involved in the recruitment of monocytes to a developing lesion area [114]. Interestingly, ApoE/Akt1 double knockout mice display more severe atherosclerotic lesions than just the ApoE single knockout mice, indicating that Akt certainly plays a role in the development of the disease [116]. This would seem contradictory to my findings that activation, not loss, of Akt reduces cholesterol efflux and may promote lipid accumulation. With that being said, the Akt knockout study was a global knockout, not macrophage-specific, and it is the local uptake of lipids by macrophages that has the most profound effect on the development of the disease.

I have shown that Akt is indeed activated in response to our FFA treatment, but the mechanism by which it achieves this is as yet unknown. FFA are known to be potent transcriptional regulators, and so there could be a change in gene expression of an upstream kinase of Akt, resulting in an increase of phosphorylation events. Another possibility is that the FFA are being incorporated into either the cell membrane, or into the PIP3 secondary messengers responsible for Akt translocation along with its upstream kinases, PDK1 and mTORC2. If the FFA are being incorporated into the cell membrane, they could be influencing the fluidity, and therefore the protein content of the local area. It is known that lipid rafts contain a different lipid composition and tend to be associated

with membrane signaling proteins [49, 50]. It is important to note that Akt activation occurs at the cell membrane. Indeed, constitutive activation of Akt is achieved by myristoylation of the kinase, which keeps it constantly attached to the cell membrane [115]. An alteration in the membrane that encouraged interaction of Akt could account for the increase in phosphorylation. If the FFA are being incorporated into PIP3, it is possible they could become a preferential binding partner for Akt or its upstream kinases, which would achieve the same result: increased time spent at the cell membrane for phosphorylation events to occur.

I have found that Akt responds quickly to our FFA treatment (Figures 8 & 9), which may lend more support to the hypothesis that direct incorporation of FFAs could be the cause of the phosphorylation, rather than through transcriptional regulation. However, additional studies at even shorter time points aimed at finding the earliest sign of activation, could be useful. The dose-dependent relationship shown between FFA concentration and extent of Akt phosphorylation (Figure 7) could be an indicator that physiological conditions could exacerbate the effects seen in the majority of these studies. The lipoproteins isolated for our experiments are from normolipidemic subjects, and therefore the FFA mixture used represents that of a healthy individual without excess plasma lipid. If the concentration of FFA released by LPL inside a growing lesion falls on the higher end of a physiological range, our study suggests that Akt would be more strongly activated, and hence the downstream effects our laboratory has shown could be more robust. Physiological levels of FFA have been recorded up to 2 mM (with a normal range between 0.5 and 0.9 mM), whereas most of our studies have used 0.68 mM, and

have still seen a significant effect on Akt phosphorylation. I have shown that at a concentration of 1.36 mM FFA (still less than the upper level of the physiological range), the phosphorylation of Akt is higher than for the 0.68 mM (or normophysiological) dose, so the potential for a more robust response in an *in vivo* situation exists [116].

Throughout this work, the serine-473 phosphorylation site of Akt was the most often assessed for activation of Akt. However, in both the initial LPL hydrolysis study in this laboratory, and in this body of work, the threonine-308 phosphorylation site has also been activated by our FFA mixture (Figure 9). While typically both sites must be phosphorylated for a fully active Akt, they are modified by two distinct kinases, and may be regulated differently [117]. Indeed, in some cancer cell types, Thr-308 seems to be the primary source of Akt activation, despite the fact that in most systems, the Ser-473 site is more important [117]. Because of this, I chose to evaluate both sites of Akt following the FFA treatment (Figures 8 & 9). We can see that there are some differences in the phosphorylation pattern of the two sites in my system, both sites were phosphorylated by approximately 200% of control levels at the 10- and 15-minute treatment times, and both sites displayed a slow reduction in pAkt over the course of 18 hours, though remaining above control.

4.2 Ability of MUFA, specifically palmitoleate, to modulate Akt activity

An interesting finding of my study was that a single FFA from the subset released by LPL, palmitoleate, was sufficient to induce the activation of Akt in the THP-1 macrophages (Figure 11). The same theories about how FFA in general could be influencing Akt apply here, but this gives us a more straightforward way to begin

assessing them, as only one FFA need be tested for a preliminary mechanistic study. There are studies that have shown the activation of Akt by MUFA (though in this case, oleate, not palmitoleate), via the blocking of an upstream inhibitor of Akt, protein tyrosine phosphatase 1B [118]. While this study showed no link between palmitoleate and Akt, the study was done in fibroblasts, not macrophages, so it could still be useful to evaluate the interactions of FFA with kinases upstream of Akt in our model.

4.3 MUFA are able to influence cholesterol efflux to apoA-I

In a meta-analysis performed in 2009 evaluating the effects of certain types of fat on cardiovascular outcomes, it was suggested that replacing the SFA in the diet with PUFA or MUFA could improve outcomes [17]. The authors hypothesis was initially that either MUFA or PUFA could improve CVD risk when compared to SFA, but were surprised to find no association with MUFA. They pointed out that most of the dietary MUFA in these studies was derived from animal fat and cited that as a possible confounding factor in their conclusion [17]. However, my data suggests that MUFA in atherosclerotic plaques may actually be an accelerating factor by partially blocking cholesterol efflux (Figure 14). A study in mouse macrophages has found that unsaturated free fatty acids (including palmitoleate) were able to reduce cholesterol efflux, in part through the reduction of apoA-I binding to the cell surface. Investigations into the rate of degradation of ABCA1 have been performed as a link to a possible mechanism, and found that unsaturated FFA accelerated the breakdown of mature ABCA1 [119]. It has been found that cyclic AMP (cAMP) increases ABCA1 expression and promotes cholesterol efflux, in part by making the protein more stable [120]. There may be

crosstalk between the protein kinase A/cAMP pathway and the PI3K/Akt pathway that allows for our FFA treatment to influence cAMP levels, though this remains to be investigated.

4.4 Cholesterol efflux to apoA-I is partially modulated by Akt, though not through transcriptional regulation of select cholesterol transport genes

The changes in the gene expression of cholesterol transporters following treatment with the FFA mixture (Figure 16) observed in this study were modest, especially when compared to earlier studies of our model [100]. Previous work has shown a robust and significant decrease of *ABCA1*, *ABCG1*, and *SCARB1* following FFA treatment [100], while in this study, only the expression of *ABCG1* was significantly reduced, with the other two genes only showing a trend. Some of these discrepancies could be explained by the difference in replicates, as the previous study had a far greater number. Overall, studies in our laboratory have indicated that the FFA released from LPL do alter cholesterol handling in the cells, and may at least partially be realized at the transcriptional level. However, there was no difference between the FFA-treated group and the FFA + MK-2206-treated group in this study, indicating no effect of Akt inhibition on the expression of cholesterol-associated genes. This is consistent with the findings of another group, who have found that Akt has no effect on the gene expression of cholesterol transporters in other cell types [122]. Interestingly, they found that PI3K activation increased cholesterol efflux to ABCA1 in hepatocytes, which is contrary to the evidence I present here. This discrepancy can likely be explained by the difference in cell model, however, as hepatocytes and macrophages have very different physiological roles

as far as metabolising and regulating cholesterol in the body. The mechanism for the influence of PI3K on cholesterol efflux in hepatocytes is based on not the overall expression of cholesterol transporters, but specifically on the cell-surface expression of them. PI3K activation induced the translocation of ABCA1 to the cell membrane, which allowed for more exchange of lipid [121]. It could be worth investigating if a similar form of regulation occurs in our macrophage model.

Though in my THP-1 model I did not see an effect of inhibiting Akt on the transcription of cholesterol transport genes, these studies indicate that the mechanism by which Akt influences cholesterol efflux is likely at the post-translational regulatory level. Other groups have looked at the potential influence of Akt on cholesterol efflux, and have found similar results to our study. For example, it has been shown that in RAW 264.7 mouse macrophages that inhibition of Akt increased ABCA1-mediated cholesterol efflux to apoA-I [95]. In addition, this effect could be attributed to a downstream component of the PI3K/Akt pathway, mTORC1. When mTORC1 was directly inhibited, cholesterol efflux also increased, which reveals a potential downstream effector for the role of Akt in macrophage lipid handling [95].

4.5 Future perspectives

Further parameters of lipid accumulation should be assessed in our research group's THP-1 macrophage system upon treatment with the FFA mixture. In particular, a theory my laboratory has postulated in the past is that these FFA are able to activate Akt by virtue of modifying the PIP3 secondary messenger molecules responsible for the translocation of Akt and its direct upstream kinases (PDK1 and mTORC2) to the cell

membrane for activation [99]. We believe that our FFA may be incorporated into these PIP3, thereby creating a preferential substrate for Akt, increasing the frequency of membrane interactions, and therefore phosphorylation. Recent experiments performed in our laboratory have been conducted to assess the changes in PIP lipid species following treatment with palmitoleate. These have demonstrated that there is an apparent incorporation of palmitoleate (16:1) into PIP biosynthesis, with significant increases in 34:1 (likely 18:0/16:1) and 34:2 (likely 18:1/16:1) PIP2 and 34:2 PIP3. While there remains more to elucidate about the mechanism of activation, this shows a proof-of-principle for the ability of FFA to alter secondary lipid messenger species [Wakelam & Brown, unpublished].

The present study has looked at inhibition of Akt as a way to establish a link between this kinase and LPL-associated changes in macrophage lipid handling. However, to strengthen this link, similar studies with an overexpression of Akt could be performed. An adenoviral construct containing myristoylated Akt has been developed by Fujio *et al.* [122], and was generously sent to our laboratory by Dr. Jason Dyck (University of Alberta) in a collaborative effort to further assess the effect of modulation of Akt in our model. Akt with this myristate post-translational modification is constitutively active within cells, by virtue of being almost completely membrane-bound, and therefore in constant proximity to its upstream effectors [115, 123]. This virus has been grown up in HEK-293T cells in our laboratory, and the virus-containing media collected for future use. This will no doubt help to elucidate the role of Akt in lipid accumulation and cholesterol efflux, as future experiments assess the role of hyper-expressed Akt.

Additionally, future work with this project would aim to determine through which possible signaling axis Akt is having these lipid modulating effects. A likely starting point could be through mTORC1 regulation, as it was shown by another research group to influence cholesterol efflux from mouse macrophages [95].

4.6 Overall conclusion

Lipoprotein lipase generates a select complement of FFA species following incubation of the enzyme with total human lipoproteins. In the present study, I have demonstrated that these FFA, at a physiologically relevant dose, may activate the signaling molecule Akt in a dose- and time-dependent manner in human THP-1 macrophages. Further, a single monounsaturated FFA, palmitoleate, seems to be responsible for most of the effects I have seen. Treatment of THP-1 macrophages with either the full complement of FFA, or palmitoleate singly (at physiological concentrations) impair cholesterol efflux to apoA-I. This effect was eliminated upon treatment with an Akt inhibitor, indicating that this process is mediated by the PI3K/Akt pathway. This is further supported by preliminary work in our laboratory that has shown inhibition of PI3K to reduce FFA-mediated neutral lipid accumulation in our model [Courage & Brown, unpublished]. While these effects on cholesterol transport may not be controlled at the transcriptional level, there are promising theories to investigate in the future to further elucidate this apparent pathway, and the pro-atherogenic role of LPL in macrophage-stimulated atherosclerosis.

References

[1] R. Ross, "The pathogenesis of atherosclerosis: a perspective for the 1990's," *Nature*, vol. 362, pp. 801-809, 1993.

[2] P. H. A. o. Canada, "Report from the Canadian Chronic Disease Surveillance System: Heart Disease in Canada, 2018," Public Health Agency of Canada, Ottawa, 2018.

[3] R. S. Padwal, A. Bienek, F. A. McAlister and N. R. C. Campbell, "Epidemiology of Hypertension in Canada: An Update," *Canadian Journal of Cardiology,* vol. 32, pp. 687-694, 2016.

[4] E. J. Benjamin, S. S. Virani, C. W. Callaway, A. M. Chamberlain, A. R. Chang, S. Cheng, S. E. Chiuve, M. Cushman, F. N. Delling, R. Deo, S. D. de Ferranti, J. F. Ferguson, M. Fornage, C. Gillespie, C. R. Isasi, M. C. Jimenez, L. C. Jordan and S. E. Judd, "Heart disease and stroke statistics-2018 update: a report from the American Heart Association," *Circulation,* vol. 137, pp. e67-e492, 2018.

[5] W. Herrington, B. Lacey, P. Sherliker, J. Armitage and S. Lewington, "Epidemiology of atherosclerosis and the potential to reduce the global burden of atherothrombotic disease," *Circulation Research,* vol. 118, pp. 535-546, 2016.

[6] J. Tarride, M. Lim, M. DesMeules, W. Luo, N. Burke, D. O'Reilly, J. Bowen and R. Goeree, "A review of the cost of cardiovascular disease," *The Canadian Journal of Cardiology,* vol. 25, pp. 195-202, 2009.

[7] S. Barquera, A. Pedroza-Tobias, C. Medina, L. Hernandez-Barrera, K. Bibbins-Domingo, R. Lozano and A. E. Moran, "Global overview of the epidemiology of atherosclerotic cardiovascular disease," *Archives of Medical Research,* vol. 46, pp. 328-338, 2015.

[8] W. Slijkhuis, W. Mali and Y. Appelman, "A historical perspective towards a non-invasive treatment for patients with atherosclerosis," *Netherlands Heart Journal,* vol. 17, pp. 140-144, 2009.

[9] C. G. Caro, "Discovery of the role of wall shear in atherosclerosis," *Arteriosclerosis, Thrombosis, and Vascular Biology,* vol. 29, pp. 158-161, 2009.

[10] S. Saltykow, "Die experimentell erzeugten Arterienveranderungen in ihrer Beziehung zu Atherosklerose und verwandten Krankheiten des-Menschen," *Zentralbl Allgem Pathol Pathol Anat,* vol. 19, pp. 321-368, 1908.

[11] I. Adler, "Studies in experimental atherosclerosis: a preliminary report," *The Journal of Experimental Medicine,* vol. XX, pp. 93-106, 1914.

[12] C. A. McMahan, S. S. Gidding, G. T. Malcom, R. E. Tracy, J. P. Strong and H. C. J. McGill, "Pathobiological determinants of atherosclerosis in youth risk scores are associated with early and advanced atherosclerosis," *Pediatrics,* vol. 118, pp. 1447-1455, 2006.

[13] B. Uslu, Y. O. Cakmak, U. Sehirli, E. N. Keskinoz, C. E, S. Arbak and A. Yalin, "Early onset atherosclerosis of the carotid bifurcation in newborn cadavers," *Journal of Clinical and Diagnostic Research,* vol. 10, pp. AC01-AC05, 2016.

[14] P. Libby, "Inflammation in atherosclerosis," *Nature,* vol. 420, pp. 868-874, 2002.

[15] G. Tsirpanlis, "Inflammation in atherosclerosis and other conditions: a response to danger," *Kidney and Blood Pressure Research,* vol. 28, pp. 211-217, 2005.

[16] H. A. Himburg, S. E. Dowd and M. H. Friedman, "Frequency-dependent response of the vascular endothelium to pulsatile shear stress," *American Journal of Physiology,* vol. 293, pp. 645-653, 2007.

[17] M. U. Jakobsen, E. J. O'Reilly, B. L. Heitmann, M. A. Pereira, K. Balter, G. E. Fraser, U. Goldbourt, G. Hallmans, P. Knekt, S. Liu, P. Pietinen, D. Spiegelman, J. Stevens, J. Virtamo, W. C. Willett and A. Ascherio, "Major types of dietary fat and risk of coronary heart disease: a pooled analysis of 11 cohort studies," *The American Journal of Clinical Nutrition,* vol. 89, pp. 1425-1432, 2009.

[18] E. A. Podrez, H. M. Abu-Soud and S. L. Hazen, "Myeloperoxidase-generated oxidants and atherosclerosis," *Free Radical Biology & Medicine,* vol. 28, pp. 1717-1725, 2000.

[19] D. A. Chistiakov, Y. V. Bobryshev and A. N. Orekhov, "Macrophage-mediated cholesterol handling in atherosclerosis," *Journal of Cellular and Molecular Medicine,* vol. 20, pp. 17-28, 2015.

[20] A. V. Finn, M. Nakano, J. Narula, F. D. Kolodgie and R. Virmani, "Concept of vulnerable/unstable plaque," *Arteriosclerosis, Thrombosis, and Vascular Biology,* vol. 30, pp. 1282-1292, 2010.

[21] A. B. Ouweneel and M. Van Eck, "Lipoproteins as modulators of atherothrombosis: from endothelial function to primary and secondary coagulation," *Vascular Pharmacology,* vol. 82, pp. 1-10, 2016.

[22] R. W. Mahley, T. L. Innerarity, S. C. Rall and K. H. Weisgraber, "Plasma lipoproteins: apolipoprotein structure and function," *Journal of Lipid Research,* vol. 25, pp. 1277-1294, 1984.

[23] F. Carmena, P. Duriez and J.-C. Fruchart, "Atherogenic lipoprotein particles in atherosclerosis," *Circulation,* vol. 109, pp. III-2 - III-7, 2004.

[24] R. W. Mahley, "Apolipoprotein E: cholesterol transport protein with expanding role in cell biology," *Science,* vol. 240, pp. 622-630, 1988.

[25] J. P. Segrest, M. K. Jones, H. De Loof and N. Dashti, "Structure of apolipoprotein B-100 in low density lipoproteins," *Journal of Lipid Research,* vol. 42, pp. 1346-1367, 2001.

[26] W. P. Castelli, R. J. Garrison and P. W. F. Wilson, "Incidence of coronary heart disease and lipoprotein cholesterol levels: The Framingham Study," *Journal of the American Medical Association,* vol. 256, pp. 2835-2838, 1986.

[27] H. M. Rubins, S. J. Robins, D. Collins, C. L. Fye, J. W. Anderson, M. B. Elam, F. H. Faas, E. Linares, E. J. Schaefer, G. Schectman, T. J. Wilt and J. Wittes, "Gemfibrozil for the secondary prevention of coronary heart disease in men with low levels of high-density lipoprotein cholesterol," *The New England Journal of Medicine,* vol. 341, pp. 410-418, 1999.

[28] D. B. Zilversmit, "Atherogenesis: a postprandial phenomenon," *Circulation ,* vol. 60, pp. 473-485, 1979.

[29] A. S. Lindman, M. B. Veierod, A. Tverdal, J. I. Pedersen and R. Selmer, "Nonfasting triglycerides and risk of cardiovascular death in men and women from the Norwegian Countries Study," *European Journal of Epidemiology,* vol. 25, pp. 789-798, 2010.

[30] K. J. Moore and I. Tabas, "Macrophages in the pathogenesis of atherosclerosis," *Cell,* vol. 145, pp. 341-355, 2011.

[31] C. S. Robbins, I. Hilgendorf, G. F. Weber, I. Theurl, Y. Iwamoto, J. Figueiredo, R. Gorbatov, G. K. Sukhova, L. M. S. Gerhardt, D. Smyth, C. C. J. Zavitz, E. A. Shikatani, M. Parsons, N. Rooijen, H. Y. Lin, M. Husain, P. Libby, M. Nahrendorf, R. Weissleder and Swirsk, "Local proliferation dominates lesional macrophage accumulation in atherosclerosis," *Nature Medicine,* vol. 19, pp. 1166-1172, 2013.

[32] K. Nakajima, T. Nakano and A. Tanaka, "The oxidative modification hypothesis of atherosclerosis: The comparison of atherogenic effects on oxidized LDL and remnant lipoproteins in plasma," *Clinica Chimica Acta,* vol. 367, pp. 36-47, 2006.

[33] S. Nozaki, H. Kashiwagi, S. Yamashita, T. Nakagawa, B. Kostner, Y. Tomiyama, A. Nakata, M. Ishigami, J. I. Miyagawa, K. Kameda-Takamura, Y. Kurata and Y. Matsuzawa, "Reduced uptake of oxidized low density lipoproteins in monocyte-derived macrophages from CD36-deficient subjects," *Journal of Clinical Investigation,* vol. 96, pp. 1859-1865, 1995.

[34] S. Allahverdian, A. C. Chehroudi, B. M. McManus, T. Abraham and G. A. Francis, "Contribution of intimal smooth muscle cells to cholesterol accumulation and macrophage-like cells in human atherosclerosis," *Circulation,* vol. 129, pp. 1551-1559, 2014.

[35] R. Wayhs, A. Zelinger and P. Raggi, "High coronary artery calcium scores pose an extremely elevated risk for hard events," *Journal of the American College of Cardiology,* vol. 39, pp. 225-230, 2002.

[36] N. Mody, Y. Tintut, K. Radcliff and L. L. Demer, "Vascular calcification and its relation to bone calcification: possible underlying mechanisms," *American Society of Nuclear Cardiology,* vol. 10, pp. 177-183, 2003.

[37] A. Manea, S.-A. Manea, A. M. Gan, A. Constantin, I. M. Fenyo, M. Raicu, H. Muresian and M. Simionescu, "Human monocytes and macrophages express NADPH oxidase 5; a potential source of reactive oxygen species in atherosclerosis," *Biochemical and Biophysical Research Communications,* vol. 461, pp. 172-179, 2015.

[38] C.-C. Hsieh, M.-H. Yen, C.-H. Yen and Y.-T. Lau, "Oxidized low density lipoprotein induces apoptosis via generation of reactive oxygen species in vasular smooth muscle cells," *Cardiovascular Research,* vol. 49, pp. 135-145, 2001.

[39] K. J. Rayner, "Cell death in the vessel wall: the good, the bad, the ugly," *Arteriosclerosis, Thrombosis, and Vascular Biology,* vol. 37, pp. 75-81, 2017.

[40] J. Lin, H. Li, M. Yang, J. Ren, Z. Huang, F. Han, J. Huang, J. Ma, D. Zhang, Z. Zhang, J. Wu, D. Huang, M. Qiao, G. Jin, Q. Wu, Y. Huang, J. Du and J. Han, "A role of RIP3-mediated macrophage necrosis in atherosclerosis development," *Cell Reports,* vol. 3, pp. 200-210, 2013.

[41] W. Martinet, D. M. Schrijvers and G. R. Y. De Meyer, "Pharmacological modulation of cell death in atherosclerosis: a promising approach towards plaque stabilization?," *British Journal of Pharamcology,* vol. 164, pp. 1-13, 2011.

[42] Y. Yamauchi and M. A. Rogers, "Sterol metabollism and transport in atherosclerosis and cancer," *Frontiers in Endocrinology,* vol. 9, p. doi: 10.3389/fendo.2018.00509, 2018.

[43] D. M. Klass, K. Buhrmann, G. Sauter, M. Del Puppo, J. Schiebner, M. Fuchs and E. F. Stange, "Biliary lipids, cholesterol and bile synthesis: different adaptive mechanisms to dietary cholesterol in lean and obese subjects," *Alimentary Pharmacology & Therapeutics,* vol. 23, pp. 895-905, 2006.

[44] J. M. Dietschy, "Regulation of cholesterol metabolism in man and in other species," *Klin Wochenschr,* vol. 62, pp. 338-345, 1984.

[45] R. A. Moreau, B. D. Whitaker and K. B. Hicks, "Phytosterols, phytostanols, and their conjugates in foods: structural diversity, quantitative analysis, and health-promoting uses," *Progress in Lipid Research,* vol. 41, pp. 457-500, 2002.

[46] M. L. Fernandez and M. Calle, "Revisiting dietary cholesterol recommendations: does the evidence support a limit of 300mg/d?," *Current Atherosclerosis Reports,* vol. 12, pp. 377-383, 2010.

[47] M. S. Brown and J. L. Goldstein, "The SREBP pathway: regulation of cholesterol metabolism by proteolysis of a membrane-bound transcription factor," *Cell,* vol. 89, pp. 331-340, 1997.

[48] G. van Meer, D. R. Voelker and G. W. Feigenson, "Membrane lipids: where they are and how they behave," *Nature Reviews Molecular Cell Biology,* vol. 9, pp. 112-124, 2008.

[49] O. G. Mouritsen and M. J. Zuckermann, "What's so special about cholesterol?," *Lipids,* vol. 39, pp. 1101-1113, 2004.

[50] D. A. Brown and J. K. Rose, "Sorting of GPI-anchored proteins to glycolipid-enriched membrane subdomains during transport to the apical cell surface," *Cell,* vol. 68, pp. 533-544, 1992.

[51] S. W. Altmann, H. R. Davis, L. Zhu, X. Yao, L. M. Hoos, G. Tetzloff, S. P. N. Iyer, M. Maguire, A. Golovko, M. Zeng, L. Wang, N. Murgolo and M. P. Graziano, "Niemann-Pick C1 like 1 protein is critical for intestinal cholesterol absorption," *Science,* vol. 303, pp. 1201-1204, 2004.

[52] T. S. Mikkola, M. S. Anthony, T. B. Clarkson and R. W. St. Clair, "Serum cholesterol efflux potential is an independent predictor of coronary artery atherosclerosis," *Atherosclerosis,* vol. 170, pp. 31-38, 2003.

[53] D. W. Russell, "The enzymes, regulation, and genetics of bile acid synthesis," *Annual Reviews of Biochemistry,* vol. 72, pp. 137-174, 2003.

[54] P. J. Barter, M. Coulfield, M. Eriksson, S. M. Grundy, J. J. Kastelein, M. Komajda, J. Lopez-Sendon, L. Mosca, J. C. Tardif, D. D. Waters, C. L. Shear, J. H. Revkin, K. A. Buhr, M. R. Fisher, A. R. Tall and B. Brewer, "Effects of torcetrapib in patients at high risk for coronary events," *The New England Journal of Medicine,* vol. 357, pp. 2109-2122, 2007.

[55] A. V. Khera, M. Cuchel, M. Llera-Moya, A. Rodrigues, M. F. Burke, K. Jafri, B. C. French, J. A. Phillips, M. L. Mucksavage, R. L. Wilensky, E. R. Mohler, G. H. Rothblat and D. J. Rader, "Cholesterol effux capacity, high-density lipoprotein function, and atherosclerosis," *The New England Journal of Medicine,* vol. 364, pp. 127-135, 2011.

[56] K. J. Rayner, F. J. Sheedy, C. C. Esau, F. N. Hussain, R. E. Temel, S. Parathath, J. M. van Gils, A. J. Rayner, A. N. Chang, Y. Suarez, C. Fernandez-Hernando, E. A. Fisher and K. J. Moore, "Antagonism of miR-33 in mice promotes reverse cholesterol transport and regression of atherosclerosis," *Journal of Clinical Investigation,* vol. 121, pp. 2921-2931, 2011.

[57] D. K. Nomura and J. E. Casida, "Lipases and their inhibitors in health and disease," *Chemico-Biological Interactions,* vol. 259, pp. 211-222, 2016.

[58] F. Beisson, A. Tiss, C. Riviere and R. Verner, "Methods for lipase detection and assay: a critical review," *European Journal of Lipid Science and Technology,* vol. 102, pp. 133-153, 2000.

[59] W. A. Hide, L. Chan and W.-H. Li, "Structure and evolution of the lipase superfamily," *Journal of Lipid Research,* vol. 33, pp. 167-178, 1992.

[60] R. J. Brown and D. J. Rader, "Lipases as modulators of atherosclerosis in murine models," *Current Drug Targets,* vol. 8, pp. 1307-1319, 2007.

[61] M. J. Walters and S. P. Wrenn, "Mechanistic roles of lipoprotein lipase and sphingomyelinase in low density lipoprotein aggregation," *Journal of Colloid and Interface Science,* vol. 363, pp. 268-274, 2011.

[62] H. L. Dicheck, K. Qian and N. Argrawal, "Divergent effects of the catalytic and bridging functions of hepatic lipase on atherosclerosis," *Arteriosclerosis, Thrombosis, and Vascular Biology,* vol. 24, pp. 1696-1702, 2004.

[63] T. Ishida, S. Choi, R. K. Kundu, K.-i. Hirata, E. M. Rubin, A. D. Cooper and T. Quertermous, "Endothelial lipase is a major determinant of HDL level," *Journal of Clinical Investigation,* vol. 111, pp. 347-355, 2003.

[64] M. Jaye, K. J. Lynch, J. Krawiec, D. Marchadier, C. Maugeais, K. Doan, V. South, M. Perrone and D. J. Rader, "A novel endothelial-derived lipase that modulates HDL metabolism," *Nature Genetics,* vol. 21, pp. 424-428, 1999.

[65] Z.-S. Ji, H. L. Dichek, R. D. Miranda and R. W. Mahley, "Heparan sulfate proteoglycans participate in hepatic lipase and apolipoprotein E-mediated binding and uptake of plasma lipoproteins, including high density lipoproteins," *Journal of Biological Chemistry,* vol. 272, pp. 31285-31292, 1997.

[66] B. M. Coady, J. D. Marshall, L. E. Hattie, A. M. Brannan, M. N. Fitzpatrick, K. E. Hickey, S. Wallin, V. Booth and R. J. Brown, "Characterization of a peptide containing the major heparin binding domain of human hepatic lipase," *Journal of Peptide Science,* vol. 24, p. e3123, 2018.

[67] A. Nicoll and B. Lewis, "Evaluation of the roles of lipoprotein lipase and hepatic lipase in lipoprotein metabolism: in vivo and in vitro studies in man," *European Journal of Clinical Investigation,* vol. 10, pp. 487-495, 1980.

[68] R. Savonen, M. Hiden, M. Hultin, R. Zechner, S. Levak-Frank, G. Olivecrona and T. Olivecrona, "The tissue distribution of lipoprotein lipase determines where chylomicrons bind," *J. Lipid Res.,* vol. 56, pp. 588-598, 2015.

[69] R. Zechner, "The tissue-specific expression of lipoprotein lipase: implications for energy and lipoprotein metabolism," *Current Opinion in Lipidology,* vol. 8, pp. 77-88, 1997.

[70] J. E. A. Braun and D. L. Severson, "Regulation of the synthesis, processing and translocation of lipoprotein lipase," *Biochemical Journal,* vol. 287, pp. 337-347, 1992.

[71] P. He, T. Jiang, X. OuYang, Y. Liang, J. Zou, Y. Wang, Q. Shen, L. Liao and X. Zheng, "Lipoprotein lipase: biosynthesis, regulatory factors, and its role in atherosclerosis and other diseases," *Clinica Chimica Acta,* vol. 480, pp. 126-137, 2018.

[72] M. Peterfy, O. Ben-Zeev, H. Z. Mao, D. Weissglass-Volkov, B. E. Aouizerat, C. R. Pullinger, P. H. Frost, J. P. Kane, M. J. Malloy, K. Reue, P. Pajukanta and M. H. Doolittle, "Mutations in LMF1 cause combined lipase deficiency and severe hypertriglyceridemia," *Nature Genetics,* vol. 39, pp. 1483-1487, 2007.

[73] K. K. Kristensen, S. R. Midtgaard, S. Mysling, O. Kovrov, L. B. Hansen, N. Skar-Gisllinge, A. P. Beigneux, B. B. Kragelund, G. Olivercrona, S. G. Young, T. J. D. Jorgensen, L. G. Fong and M. Ploug, "A disordered acidic domain in GPIHBP1 harboring a sulfated tyrosine regulates lipoprotein lipase," *PNAS,* vol. 115, pp. E6020-E6029, 2018.

[74] Y. Kobayashi, T. Nakajima and I. Inoue, "Molecular modeling of the dimeric structure of human lipoprotein lipase and functional studies of the carboxyl-terminal domain," *European Journal of Biochemistry,* vol. 269, pp. 4701-4710, 2002.

[75] H. Tilbeurgh, A. Roussel, J.-M. Lalouel and C. Cambilau, "Lipoprotein lipase molecular model based on the pancreatic lipase x-ray structure: consequences for heparin binding and catalysis," *Journal of Biological Chemistry,* vol. 269, pp. 4626-4633, 1994.

[76] C. K. Hayne, H. Yumerefendi, L. Cao, J. W. Gauer, M. J. Lafferty, B. Kuhlman, D. A. Erie and S. B. Neher, "We FRET so you don't have to: new models of the lipoprotein lipase dimer," *Biochemistry,* vol. 57, pp. 241-254, 2018.

[77] G. Birrane, A. P. Beigneux, B. Dwyer, B. Strack-Logue, K. K. Kristensen, O. L. Francone, L. G. Fong, H. D. T. Mertens, C. Q. Pan, M. Ploug, S. G. Young and M. Meiyappan, "Structure of the lipoprotein lipase-GPIHBP1 complex that mediates plasma triglyceride hydrolysis," *PNAS,* vol. 116, pp. 1723-1732, 2019.

[78] M. Reimund, M. Larsson, O. Kovrov, S. Kasvandik, G. Olivecrona and A. Lookene, "Evidence for two distinct binding sites for lipoprotein lipase on glycosylphosphatidylinositol-anchored high density lipoprotein binding protein 1 (GPIHBP1)," *Journal of Biological Chemistry,* vol. 290, pp. 13919-13934, 2015.

[79] M. Mulder, P. Lombardi, H. Jansen, T. J. C. van Berkel, R. R. Frants and L. M. Havekes, "Heparan sulfate proteoglycans are involved in the lipoprotein lipase-mediated enhancement of the cellular binding of very low denisty and low density lipoproteins," *Biochemical and Biophysical Research Communications,* vol. 185, pp. 582-587, 1992.

[80] J. Zdunek, G. V. Martinez, J. Schleucher, P. O. Lycksell, Y. Yin, S. Nilsson, Y. Shen, G. Olivecrona and S. Wijmenga, "Global structure and dynamics of human

apolipoprotein CII in complex with micelles: evidence for increased mobility of the helix involved in the activation of lipoprotein lipase," *Biochemistry,* vol. 42, pp. 1872-1889, 2003.

[81] T. A. Musliner, E. C. Church, P. N. Herbert, M. J. Kingston and R. S. Shulman, "Lipoprotein lipase cofactor activity of a carboxyl-terminal peptide of apolipoprotein C-II," *PNAS,* vol. 74, pp. 5358-5362, 1977.

[82] M. Larsson, E. Vorrsjo, P. Talmud, A. Lookene and G. Olivercrona, "Apolipoproteins C-I and C-III inhibit lipoprotein lipase activity by displacement of the enzyme from lipid droplets," *Journal of Biological Chemistry,* vol. 288, pp. 33997-34008, 2013.

[83] C. L. Malmendier, J.-F. Lontie, G. A. Grutman and C. Delcroix, "Metabolism of apolipoprotein C-III in normolipidemic human subjects," *Atherosclerosis,* vol. 69, pp. 51-59, 1988.

[84] D. B. Zilversmit, "A proposal linking atherogenesis to the interaction of endothelial lipoprotein lipase with triglyceride-rich lipoproteins," *Circulation Research,* vol. 33, pp. 633-638, 1973.

[85] J. E. Corey and D. B. Zilversmit, "Effect of cholesterol feeding on arterial lipolytic activity in the rabbit," *Atherosclerosis,* vol. 27, pp. 201-212, 1977.

[86] K. Wilson, G. L. Fry, D. A. Chappell, C. D. Sigmund and J. D. Medh, "Macrophage-specific expression of human lipoprotein lipase accelerates atherosclerosis in transgenic apolipoprotein E knockout mice but not in C57BL/6 mice," *Arteriosclerosis, Thrombosis, and Vascular Biology,* vol. 21, pp. 1809-1815, 2001.

[87] P.-P. He, X.-P. OuYang, Y. Li, Y.-C. Lv, Z.-B. Wang, F. Yao, W. Xie, Y.-L. Tan, L. Li, M. Zhang, G. Lan, D. Gong, H.-P. Cheng, H.-J. Zhong, D. Liu, C. Huang, Z.-X. Li, X.-L. Zheng, W.-D. Yin and C.-K. Tang, "MicroRNA-590 inhibits lipoprotein lipase expression and prevents aherosclerosis in apoE knockout mice," *PLoS ONE,* vol. 10, p. e0138788, 2015.

[88] G. Renier, E. Skamene, J. B. DeSanctis and D. Razioch, "Induction of tumor necrosis factor a gene experssion by lipoprotein lipase," *Journal of Lipid Research,* vol. 35, pp. 271-278, 1994.

[89] A. M. Weaver, J. J. Lysiak and S. L. Gonias, "LDL receptor family-dependent and -independent pathways for the internalization and digestion of lipoprotein lipase-

associated b-VLDL by rat vascular smooth muscle cells," *Journal of Lipid Research,* vol. 38, pp. 1841-1850, 1997.

[90] V. R. Babaev, S. Fazio, L. A. Gleaves, K. J. Carter, C. F. Semenkovich and M. F. Linton, "Macrophage lipoprotein lipase promotes foam cell formation and atherosclerosis in vivo," *Journal of Clinical Investigation,* vol. 103, pp. 1697-1705, 1999.

[91] B. D. Manning and L. C. Cantley, "Akt/PKB signaling: Navigating downstream," *Cell,* vol. 129, pp. 1261-1274, 2007.

[92] X.-d. Peng, P.-z. Xu, M.-l. Chen, A. Hahn-Windgassen, J. Skeen, J. Jacobs, D. Sundararajan, W. S. Chen, S. E. Crawford, K. G. Coleman and N. Hay, "Dwarfism, impaired skin development, skeletal muscle atrophy, delayed bone development, and impeded adipogenesis in mice lacking Akt1 and Akt2," *Genes & Development,* vol. 17, pp. 1352-1365, 2003.

[93] D. Auguin, P. Barthe, M.-T. Auge-Senegas, M.-H. Stern, M. Noguchi and C. Roumestand, "Solution structure and backbone dynamics of the pleckstrin homology domain of the human protein kinase B (PKB/Akt). Interaction with inositol phosphates," *Journal of Biomolecular NMR,* vol. 28, pp. 137-155, 2004.

[94] M. Andjelkovic, D. R. Alessi, R. Meier, A. Fernandez, N. C. J. Lamb, M. Frech, P. Cron, P. Cohen, J. M. Lucoqu and B. A. Hemmings, "Role of translocation in the activation and function of protein kinase B," *Journal of Biological Chemistry,* vol. 272, pp. 31515-31524, 1997.

[95] F. Dong, Z. Mo, W. Eid, K. C. Courtney and X. Zha, "Akt inhibition promotes ABCA1-mediated cholesterol efflux to apoA-1 through supressing mTORC1," *PLoS ONE,* vol. 9, p. e113789, 2014.

[96] A. Arcaro, M. Aubert, M. E. Espinosa del Hiero, U. K. Khanzada, S. Angelidou, T. D. Tetley, A. G. Bittermann, M. C. Frame and M. J. Secki, "Critical role for lipid raft-associated Src kinases in activation of PI3K/Akt signalling," *Cellular Signalling,* vol. 19, pp. 1081-1092, 2007.

[97] J. Daragmeh, W. Barriah, B. Saad and H. Zaid, "Analysis of PI3K components in human cancers," *Oncology Letters,* vol. 11, pp. 2913-2918, 2016.

[98] H. C, S. Wei, F. He, D. Liu, H. Wan, H. Liu, L. Li, H. Xu, X. Du and F. Xu, "The regulation of lipid deposition by insulin in goose liver cells is mediated by the PI3K/Akt/mTOR signalling pathway," *PLoS ONE,* vol. 10, p. e0098759, 2014.

[99] Y. Essaji, Y. Yang, C. J. Albert, D. A. Ford and R. J. Brown, "Hydrolysis products generated by lipoprotein lipase and endothelial lipase influence macrophage cell signalling pathways," *Lipids,* vol. 48, pp. 769-778, 2013.

[100] Y. Yang, N. Thyagarajan, B. M. Coady and R. J. Brown, "Cholesterol efflux from THP-1 macrophages is impaired by the fatty acid component from lipoprotein hydrolysis by lipoprotein lipase," *Biochemical and Biophysical Research Communications,* vol. 451, pp. 632-636, 2014.

[101] N. Thyagarajan, J. D. Marshall, A. T. Pickett, C. Schumacher, Y. Yang, S. L. Christian and R. J. Brown, "Transcriptomic analysis of THP-1 macrophages exposed to lipoprotein hydrolysis products generated by lipoprotein lipase," *Lipids,* vol. 52, pp. 189-205, 2016.

[102] R. J. Brown, F. Shao, A. Baldan, C. J. Albert and D. A. Ford, "Cholesterol efflux analyses using stable isotopes and mass spectometry," *Analytical Biochemistry,* vol. 433, pp. 56-64, 2013.

[103] P. Chomczynski and N. Sacchi, "Single-step method of RNA isolation by acid guanidinium thiocyanate-phenol-chloroform extraction," *Analytical Biochemistry,* vol. 162, pp. 156-159, 1987.

[104] M. W. Pfaffl, "A new mathematical model for relative quantification in real-time RT-PCR," *Nucelic Acids Research,* vol. 29, p. e45, 2001.

[105] J. Miyamoto, S. Hasegawa, M. Kasubuchi, A. Ichimura, A. Nakajima and I. Kimura, "Nutirional signaling via free fatty acid receptors," *International Journal of Molecular Sciences,* vol. 17, p. 450; doi:10.3390/ijms17040450, 2016.

[106] Z. Papackova and M. Cahova, "Fatty acid signaling: the new function of intracellular lipases," *International Journal of Molecular Sciences,* vol. 16, pp. 3831-3855, 2015.

[107] A. Ghosh, L. Gao, T. Abhimanyu, P. M. Siu and C. W. K. Lai, "Role of free fatty acids in endothelial dysfunction," *Journal of Biomedical Science,* vol. 24, pp. DOI 10.1186/s12929-017-0357-5, 2017.

[108] S. Oikari, T. Ahtialansaari, A. Huotari, K. Keihne, U. R. Folsch, S. Wolffram, J. Janne, L. Alhonen and K. H. Herzig, "Effect of medium- and long-chain fatty acid diets on PPAR and SREBP expression and glucose homeostasis in ACBP-overexpressing transgenic rats," *Acta Physiologica,* vol. 194, pp. 57-65, 2008.

[109] S. Kersten, J. Seydoux, J. M. Peters, F. J. Gonzalez, B. Desvergne and W. Wahli, "Peroxisome proliferator-activated receptor a mediates the adaptive response to fasting," *The Journal of Clinical Investigation*, vol. 103, pp. 1489-1498, 1999.

[110] J. Xu, G. Xiao, C. Trujillo, V. Chang, L. Blanco, S. B. Joseph, S. Bassilian, M. F. Saad, P. Tontonoz, W. N. Paul Lee and I. J. Kurland, "Peroxisome proliferator-activated receptor a (PPARa) influences substrate ultilization for hepatic glucose production," *Journal of Biological Chemistry*, vol. 277, pp. 50237-50244, 2002.

[111] M. Delmastro-Greenwood, B. A. Freeman and S. G. Wendell, "Redox-dependent anti-inflammatory signaling actions of unsaturated fatty acids," *Annual Review of Physiology*, vol. 76, pp. 79-105, 2014.

[112] T. E. Akiyama, S. Sakai, G. Lambert, C. J. Nicol, Matsusue, Kimihiko, S. Pimprale, Y.-H. Lee, M. Ricote, C. K. Glass, H. B. J. Brewer and F. J. Gonzalez, "Conditional disruption of the peroxisome proliferator-activaed receptor y gene in mice results in lowered expression of ABCA1, ABCG1, and apo E in macrophages and reduced cholesterol efflux," *Molecular and Cellular Biology*, vol. 22, pp. 2607-2619, 2002.

[113] J. Xu, M. T. Nakamura, H. P. Cho and S. D. Clarke, "Sterol regulatory element binding protein 1 expression is suppressed by dietary polyunsaturated fatty acids: A mechanism for the coordinate suppression of lipogenic genes by polyunsaturated fats," *The Journal of Biologcal Chemistry*, vol. 274, pp. 23577-23583, 1999.

[114] K. Murao, T. Ohyama, H. Imachi, T. Ishida, W. M. Cao, H. Namihira, M. Sato, N. C. W. Wong and J. Takahara, "TNF-a stimulation of MCP-1 expression is mediated by the Akt/PKB signal transduction pathway in vascular endothelial cells," *Biochemical and Biophysical Research Communications*, vol. 276, pp. 791-796, 2000.

[115] R. M. Adam, N. K. Mukhopadhyay, J. Kim, D. D. Vizio, B. Cinar, K. Boucher, K. R. Solomon and M. R. Freeman, "Cholesterol sensitivity of endogenous and myristoylated Akt," *Cancer Research*, vol. 67, pp. 6238-6246, 2007.

[116] L. C. Gormsen, J. Gjedsted, S. Gjedde, H. Norrelund, J. S. Christiansen, O. Schmitz, J. O. L. Jorgensen and N. Moller, "Dose-response effects of free fatty acids on amino acid metabolism and ureagenesis," *Acta Physiologica*, vol. 192, pp. 369-379, 2007.

[117] E. E. Vincent, D. J. E. Elder, E. C. Thomas, L. Phillips, C. Morgan, J. Pawade, M. Sohail, M. T. Tay, M. R. Hetzel and T. J. M, "Akt phosphrylation on Thr308 but

not on Ser473 correlates with Akt protein kinase activity in human non-small cell lung cancer," *British Journal of Cancer,* vol. 104, pp. 1755-1761, 2011.

[118] E. Shibata, T. Kanno, A. Tsuchiya, K. Kuribayashi, C. Tabata, T. Nakano and T. Nishizaki, "Free fatty acids inhibit protein tyrosine phosphatase 1B and activate Akt," *Cellular Physiology and Biochemistry,* vol. 32, pp. 871-879, 2013.

[119] Y. Wang and J. F. Oram, "Unsaturated fatty acids inhibit cholesterol efflux from macrophages by increasing degradation of ATP-binding cassette transporter 1," *Journal of Biological Chemistry,* vol. 277, pp. 5692-5697, 2002.

[120] B. Haidar, M. Denis, L. Krimbou, M. Marcil and J. Genest, "cAMP induces ABCA1 phosphorylation activity and promotes cholesterol efflux from fibroblasts," *Journal of Lipid Research,* vol. 43, pp. 2087-2094, 2002.

[121] C.-X. Huang, Y.-L. Zhang, J.-F. Wang, J.-Y. Jiang and J.-L. Bao, "MCP-1 impacts RCT by repressing ABCA1, ABCG1, and SR-BI through PI3K/Akt posttranslational regulation in HepG2 cells," *Journal of Lipid Research,* vol. 54, pp. 1231-1240, 2013.

[122] Y. Fujio, T. Nguyen, D. Wencker, R. N. Kitsis and K. Walsh, "Akt promotes survival of cardiomyocytes in vitro and protects against ischemia-repurfusion injury in mouse heart," *Circulation,* vol. 101, pp. 660-667, 2000.

[123] A. D. Kohn, S. A. Summers, M. J. Birnbaum and R. A. Roth, "Expression of a constitutively active akt Ser/Thr Kinase in 3T3-L1 adipocytes stimulates glucose uptake and glucose transporter 4 translocation," *The Journal of Biological Chemistry,* vol. 271, pp. 31372-31378, 1996.